



VCU

Virginia Commonwealth University
VCU Scholars Compass

Theses and Dissertations

Graduate School

2019

Restoration of Contractile Protein Expression and Colonic Smooth Muscle Function by Hydrogen Sulfide in DMD Mice

Kulpreet Singh
Virginia Commonwealth University

Follow this and additional works at: <https://scholarscompass.vcu.edu/etd>



Part of the [Medical Education Commons](#)

© The Author

Downloaded from

<https://scholarscompass.vcu.edu/etd/5790>

This Thesis is brought to you for free and open access by the Graduate School at VCU Scholars Compass. It has been accepted for inclusion in Theses and Dissertations by an authorized administrator of VCU Scholars Compass. For more information, please contact libcompass@vcu.edu.

**Restoration of Contractile Protein Expression and Colonic Smooth Muscle Function by
H₂S in Duchenne Muscular Dystrophy Mice**

A thesis submitted in partial fulfillment of the requirements for the degree of Master of Science
at Virginia Commonwealth University

by

Kulpreet Singh

Bachelor of Science, Professional Science & Biology, Virginia Commonwealth University, 2017

Director:

S. Murthy Karnam Ph.D.

Professor, Department of Physiology and Biophysics

Virginia Commonwealth University

Richmond, Virginia

April, 2019

Acknowledgements

I would like to firstly thank my parents, Kuldeep and Jasvinder Slach, as well as my sister, Angel Slach, for their undying love and support as I successfully completed all of my academic endeavors.

Now I cannot over-exaggerate the appreciation and gratitude I have for being able to learn and conduct research in one of the leading labs associated with gastrointestinal research a VCU. It has been enlightening to be able to work under such leaders in the research field. I am thankful to my fellow lab mates Adam, Molly, Gurpreet, Hangxia, and Shanwei for making such a positive work environment. Dr. Sunila Mahavadi taught me almost everything I needed to know for my project, helping me initiate my experiment on time and understand the process as I work along. As for the two greats, Dr. Karnam and Dr. Grider, what I say about them could never be enough. Dr. Karnam is probably one of the smartest people I have ever known, while being helpful and patient with his students. His sense of humor and reassurance throughout the frustrating moments I had during some experiments motivated me at every moment. As for Dr. Grider, he sets the positive culture of the lab, teaching me how to approach research, career, and life in a very easy-going, fun, yet successful manner. I am very thankful for all the memories we have made

I thank them both for their support and understanding as I tried my best to keep the centrifuge running. I hope in the future, I will be able to come back as a medical student and physician and be able to learn other valuable lessons from their lab again.

Table of Contents

	Page
<i>Acknowledgements.</i>	2
<i>List of Figures</i>	5
<i>Abstract</i>	7
<i>Chapter 1: Introduction</i>	
<i>1.1: Background Duchenne Muscular Dystrophy</i>	9
<i>1.2: Dystrophin Introduction- Background, Function, and Pathogenesis</i>	10
<i>1.3: Dystrophin in Skeletal Muscle</i>	12
<i>1.4: Dystrophin in Cardiac Muscle</i>	13
<i>1.5: Dystrophin in Smooth Muscle</i>	14
<i>1.6: Overview of Gastrointestinal Tract Function and Anatomy</i>	16
<i>1.7: Anatomy of Gastrointestinal Wall</i>	17
<i>1.8: Motility Functions of the Colon (Large Intestine)</i>	18
<i>1.9: Smooth Muscle Structure with Contractile Protein Emphasis</i>	19
<i>1.10: Excitation-Contraction Coupling and Thin Filament Associated Proteins</i>	20
<i>1.11: Excitation-Transcription Coupling</i>	24
<i>1.12: Muscular Dystrophy-Abnormal GI Motility</i>	25
<i>1.13: Oxidative Stress</i>	26
<i>1.14: Hydrogen Sulfide (H₂S)</i>	27
<i>1.15: Mouse Models of mdx</i>	29
<i>1.16: Rationale</i>	30
<i>Chapter 2: Materials and Methods</i>	
<i>2.1: Reagents</i>	32
<i>2.2: Animals</i>	32

2.3: <i>H₂S Treatment</i>	33
2.4: <i>Collection/Preparation of Colonic Tissue</i>	33
2.5: <i>Preparation of Dispersed Smooth Muscle Cells</i>	34
2.6: <i>Measurements of Contraction in Muscle Strips</i>	35
2.7: <i>Measurement of Contraction in Dispersed Smooth Muscle Cells</i>	35
2.8: <i>Qualitative Real-Time PCR Analysis (qRT-PCR)</i>	36
2.9: <i>Western Blot Analysis</i>	37
2.10: <i>Statistical Analysis</i>	38
<i>Chapter 3: Results</i>	
3.1: <i>Effect of DMD on Smooth Muscle Contraction and Relaxation</i>	39
3.2: <i>Changes in Expression of Thin-Filament Associated Proteins</i>	43
<i>Chapter 4: Discussion</i>	50
<i>References</i>	65

List of Figures

<i>1: Diagram of Dystrophin</i>	12
<i>2: Schematic of Smooth Muscle Contraction Signaling</i>	21
<i>3: Ach-Induced Contraction in Colonic Muscle Strips of Mdx Mice</i>	46
<i>4: Ach-Induced Contraction in Colonic Muscle Strips of mdx/mTR mice and the effect of H₂S Treatment on Smooth Muscle Contraction</i>	47
<i>5: SNP-induced Relaxation in Colonic Muscle Strip of Mdx Mice</i>	48
<i>6: SNP-induced relaxation in Colonic Muscle Strips of Mdx/mTR mice and H₂S Treated Mice</i>	49
<i>7: Initial Ach-Induced Contraction in Dispersed Colonic Smooth Muscle Cells</i>	50
<i>8: Sustained Ach-Induced Contraction in Dispersed Colonic Smooth Muscle Cells</i>	51

<i>9: SNP-Induced Relaxation in Dispersed Colonic Smooth Muscle Cells of Mdx Mice</i>	52
<i>10: ISO-Induced Relaxation in Dispersed Colonic Smooth Muscle Cells of Mdx Mice</i>	53
<i>11: mRNA and Protein Expression of Caldesmon in Colon of Mdx mice</i>	54
<i>12: mRNA Expression of Caldesmon in Colon of mdx/mTR mice and the Effect of H₂S Treatment on expression</i>	55
<i>13: mRNA and Protein Expression of Calponin in Colon of Mdx mice</i>	56
<i>14: mRNA Expression of Calponin in Colon of mdx/mTR mice and the Effect of H₂S Treatment on expression</i>	57
<i>15: mRNA and Protein Expression of Tropomyosin in Colon of Mdx mice</i>	58
<i>16: mRNA and Protein Expression of Smoothelin in Colon of Mdx Mice</i>	59

ABSTARCT

Duchenne Muscular Dystrophy (DMD), characterized by the lack of dystrophin, results from a mutation in the Xp21 gene which encodes for the protein dystrophin that links the extracellular matrix to the actin cytoskeleton in skeletal, cardiac and smooth muscle. Slow colonic transit and chronic constipation are common in DMD patients due to the weakening of the abdominal wall muscles and gut smooth muscle. However, the cause of this hypocontractility in DMD patients and the expression of contractile proteins in smooth muscle are unknown. Expression of contractile proteins is regulated by the signaling pathways activated by excitatory (e.g., acetylcholine, ACh) and inhibitory transmitters (e.g., nitric oxide). Hydrogen sulfide (H₂S) is well-known for its anti-oxidant effects; however, its utility to restore DMD-induced effects is unknown. Aim: To investigate the expression of contractile proteins and smooth muscle function in the colon of wild type mice and models of DMD (*mdx* and *mdx/mTR* mice) and the effect of H₂S on these in *mdx* mice. Methods: Contraction of colonic segments was measured in the longitudinal orientation from 3-month old control and *mdx* mice, and 9-month old control and *mdx/mTR* mice, (*mdx/mTR* exhibit increased disease severity). The effect of SG1002, an orally active slow releasing H₂S agent, was tested in *mdx/mTR* mice (40 mg/kg body weight in chow/every 3 days starting from 3 weeks to 9 months). Expression of contractile proteins was

measured by qRT-PCR and western blot. Results: Expression of smoothelin, caldesmon, calponin and tropomyosin was decreased in colonic smooth muscle of *mdx* mice compared to control. This decrease was associated with a decrease in ACh-induced contraction in colonic segments (21 ± 3 mN/100 mg tissue in control and 3 ± 1 mN/100 mg tissue in *mdx* mice). To identify the specific involvement of smooth muscle dysfunction in the decrease in contraction, colonic muscle cells were isolated and contraction in response to ACh was measured by scanning micrometry and expressed as the percent decrease in cell length from control cell length. ACh-induced contraction was also inhibited in muscle cells isolated from *mdx* mice compared to control ($43 \pm 5\%$ in control and $27 \pm 3\%$ in *mdx* mice). ACh-induced contraction was decreased in colonic segments from *mdx/mTR* mice (12 ± 2 mN/100 mg tissue in control versus 4 ± 1 mN/100 mg tissue in *mdx/mTR*) and the decrease was partly reversed by SG1002 treatment (9 ± 1 mN/100 mg tissue). mRNA expression of thin filament associated proteins was also decreased in colonic smooth muscle from *mdx/mTR* mice and the decrease was reversed by SG1002. These results suggest that H₂S restores contractile protein mRNA expression and contraction in *mdx/mTR* mice. Conclusion: The data indicate that the lack of dystrophin in *mdx* mice adversely affects colonic smooth muscle contractility through the down regulation of contractile protein mRNA expression. Treatment of *mdx/mTR* mice with H₂S restores contractile phenotype. Thus, H₂S treatment would be an area of study in therapeutic control of DMD-induced gastrointestinal motility disorders.

Chapter 1: INTRODUCTION

1.1: Background Duchenne Muscular Dystrophy

Duchenne Muscular Dystrophy (DMD) is a rapidly progressive neuromuscular and X-linked disorder that affects 15.9 to 19.5 per 100,000 live births, characterized by muscle weakness with eventual disability (Yucel et al., 2018) (Ryder et al.2017). It is caused by mutations in the gene located at Xp21, which encodes for the protein dystrophin. Continuous muscular damage and muscle fiber degeneration is evident in patients suffering from DMD, causing muscular weakness that is associated with motor delays, loss of ambulation, respiratory impairment and cardiomyopathy (Birnkrant et al., 2018). Effects of this genetic disorder are apparent in individuals early on from ages 1-3 through symptoms such as delayed walking, frequent falls, and difficulty climbing stairs due to the effects that a lack of dystrophin has on the muscular system (Ryder et al.2017). In terms of the gastro-intestinal system, chronic constipation is highly prevalent and an ongoing

source of discomfort and distress in DMD patients- this is specifically due to the struggles of GI motility caused by the manifestation of the DMD phenotype on gastrointestinal smooth muscle (Brumbaugh et al., 2018) (Lo Cascio et al., 2016). Chronic constipation in DMD patients requires the regular use of laxatives and enemas, promoting life-threatening metabolic acidosis through the loss of bicarbonate, furthering the complications associated with the consequences of DMD (Lo Cascio et al., 2014). Most people with DMD die from cardiac failure before or during their 30s as the cardiomyopathy that develops in DMD causes the heart chambers of individual to enlarge and the walls to thin out, ultimately leading to the development of heart failure (Ryder et al., 2017). Although death is inevitable, the gastrointestinal effects of DMD result in a very poor quality of life for patients suffering from the disease.

1.2: Dystrophin Introduction- Background, Function, and Pathogenesis

DMD is caused by mutations in the gene that encodes for the 427-kD cytoskeleton protein dystrophin (Nowak & Davies 2004). The dystrophin gene is the largest in the human genome, consisting of 2.6 million base pairs of DNA and 79 exons. The full-length dystrophin isoform, dp427, is generated from three distinct, tissue specific promoters: the (M) muscle type promoter that drives expression of dystrophin in all three muscle groups, the brain-type (B) promoter that drives dystrophin expression in cortical and cerebellar neurons and the heart, and the purkinje type (P) promoter that drives cerebellar dystrophin expression (Petkova et al., 2016). Around 60% of the mutations of dystrophin are due to large insertions or deletions that lead to further downstream frameshift errors (Nowak & Davies 2004).

Structurally, the dystrophin protein plays a critical role in muscles in linking the intracellular actin cytoskeleton of a myocyte to the extracellular matrix via the dystrophin associated protein complex (DAPC), protecting the sarcolemma from contractile stress (Blake et al., 2002) (Petkova et al., 2016) (Petrof 2002). Dystrophin contains four main functional domains: an amino (N) terminus that connects to the intracellular F-actin cytoskeleton, the central rod domain that contains spectrin-like repeats, the cysteine rich domain, and the carboxyl terminus that binds the DAPC, providing the link between the intracellular cytoskeleton and the ECM (Guiraud et al., 2015) (Renzhi et al., 2011) (Wang et al., 2016). The spectrin-like repeats of dystrophin's rod like domain predict that dystrophin may function as a shock absorber, resisting multiple rounds of muscle contraction and relaxation (Guiraud et al., 2015). Furthermore, dystrophin itself assembles several transmembrane proteins and cytoplasmic proteins into the DPAC, which is divided into: the dystroglycan complex, sarcoglycan complex, and cytoplasmic and ECM components. Ultimately, the DAPC connects the cytoskeleton with the ECM, leading to the mechanical stability of the sarcolemma and protection against contraction-induced muscle damage (Petkova et al., 2016). The vast majority of patients with DMD completely lack dystrophin; however, even with reduction in the amount or alteration in the size of the dystrophin gene leads to a less severe type of muscular dystrophy of Becker's Muscular Dystrophy, suggesting the crucial impact dystrophin has on the muscular system (Nowak & Davies 2004).

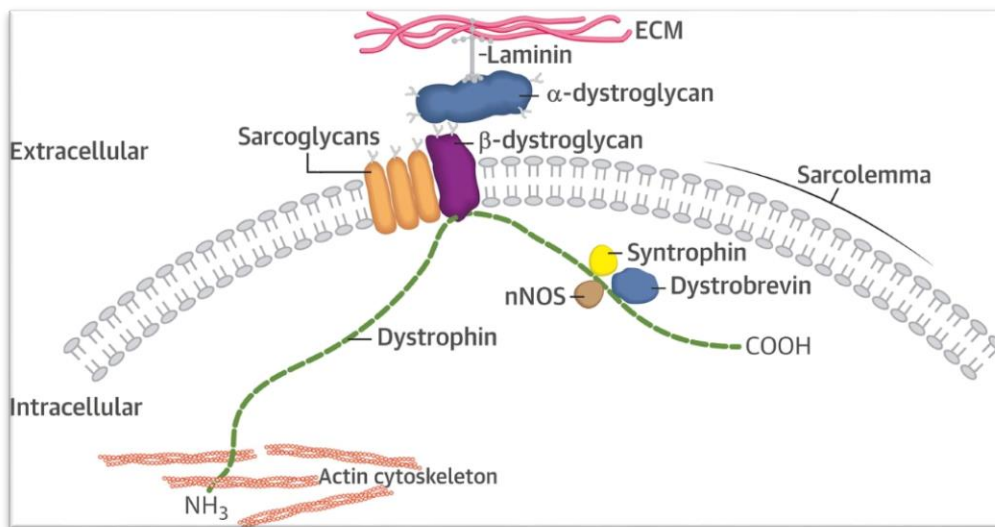


Figure 1. Diagram of Dystrophin (Kamdar 2016 JACC). Schematic diagram of DGC (dystroglycan complex). DGC is seen to span the sarcolemmal membrane and link the cytoplasmic actin cytoskeleton to the ECM via dystrophin. The DGC includes sarcoglycans, β -dystroglycan, and extracellular α -dystroglycan. Cytoplasmic components include dystrophin which binds to dystrobrevin, syntrophin, and nitric oxide synthase.

1.3: Dystrophin- Skeletal Muscle

Skeletal muscles are dynamic tissues that undergo stress from each contraction. The connection between the cytoskeleton of the muscle cell and the ECM is imperative for maintaining cellular integrity and function during each cycle of contraction and stress (Guiraud et al., 2015) (Renzhi et al., 2011) (Wang et al., 2016). In completely regular, non-affected skeletal muscles, the susceptibility for mechanical damage is ongoing; however, homeostasis is maintained through injury repair by muscle stem cells and satellite cells. In DMD, DAPC, which is responsible for the physical connection of the sarcolemmal cytoskeleton with the ECM, loses its 'structural linkage' due to the loss of dystrophin, making the sarcolemma prone to further damage by mechanical stress and leaving the repair processes incapable of maintaining homeostasis (Beyers et al., 1993). Now during contraction, there is sarcolemmal damage, an increase in membrane permeability to Ca^{++}

and small ions, leading to cell death and dysfunction. This imbalance between skeletal muscle degeneration to regeneration initiates the process of fibrosis via inflammatory processes, which is a hallmark of DMD (Guiraud et al., 2015) (Han et al., 2011). Histologically, normal skeletal muscles consist of muscle fibers that are evenly spaced, angular, and uniform in size; on the contrary, DMD muscle biopsies show necrotic and degenerative muscle fibers, with the lost muscle myofibers being replaced by connective tissue and fat (Blake et al., 2002) (Guiraud et al., 2015).

1.4: Dystrophin- Cardiac Muscle

95% of patients with DMD develop cardiomyopathies by the age of 20, and cardiac failure is one of the major sources of mortality in DMD patients, with respiratory failure being the other (Birnkrant et al., 2018) (Mourkioti et al., 2013) (Kaprielian and Severs 2000). Cardiac muscles of DMD patients either completely lack dystrophin or have a truncated version of the protein. It is understood that dystrophin plays a role in linking the cytoskeleton to the ECM via DAPC (Mourkioti et al., 2013). It is the cytoskeleton that allows cardiomyocytes to maintain their characteristic shape and structure despite the contraction-induced damage imposed on the cardiac muscle cells from the cyclic contractions of the heart (Mourkioti et al., 2013) (Kaprielian and Severs 2000) (Kuo and Ehrlich 2015).

Compared to skeletal muscles, dystrophin in cardiomyocytes is not only distributed along the sarcolemma, but also the transverse tubules, where it is not seen in the skeletal muscles (Kaprielian and Severs 2000) (Kaprielian et al., 2000) (Byers et al., 1991).

Dystrophin is also absent from the membrane that overlays the adheren junctions of the intercalated discs (Byers et al., 1991) (Kaprielian and Severs 2000).

Dystrophin's structural role in providing membrane stability and increased mechanical strength of the myocyte membrane, it is well understood that in cardiomyocytes, like in skeletal muscles, it plays an important role in regulating the force of transmission in cardiomyocytes during the cyclic process of contraction in the heart (Kaprielian and Severs 2000) (Kaprielian et al., 2000) (Shirokova and Niggli 2013). Nevertheless, the distribution of dystrophin along the T-tubules suggests that dystrophin serves roles more than just contractile force as T-tubules are not directly affected by membrane distortion during cardiac contraction (Kaprielian and Severs 2000) (Kaprielian et al., 2000).

1.5: Dystrophin- Smooth Muscle

In smooth muscle cell membranes, dystrophin is not seen to be distributed uniformly across the SMC membrane, but more distantly and discontinuously (Beyers et al., 1991) (North et al., 1993). More specifically, dystrophin is seen to be dispersed in the caveolae-rich domains of the smooth muscle cells (North et al., 1993).

During the contraction of smooth muscles, the mechanical damage from muscle contraction falls upon the sarcolemma, where just as in skeletal and cardiac muscles, dystrophin provides the mechanical support to the SMC membrane via anchorage of the cytoskeleton to the ECM. Nonetheless, the distribution of dystrophin in caveolae-rich domains predicts interaction between these two structures, suggesting that dystrophin may

also act as a tension-sensing molecule that conveys information about sarcolemmal stress to the mechanosensitive Ca^{++} channels (Beyers et al., 1991).

A distinct feature found on contractile SMCs is the abundance of caveolae, exceeding 160,000 in number on a single SMC. Caveolae contribute to mechanisms that modulate contractile and proliferative activity with SMCs. They contain caveolins that are needed for scaffolding and signal-transduction (Halayko and Stelmack 2005). Caveolin-1 attaches to the intracellular tail of B-dystroglycan, the core transmembrane subunit of the dystrophin-glycoprotein complex (DGC/DPAC), which is linked to the intracellular actin via dystrophin and ECM laminin via α -dystroglycan. Caveolin-1 and dystrophin overlap at the membrane of contractile SMCs, where one of the key roles of dystrophin/DGC is to stabilize the plasma membrane to protect it against any damaging contraction-induced force. The close association of caveolins with DGC and cytoskeleton may also play a unique role in mediating and stabilizing the ordered compartmentalization of caveolae on the plasma membrane (North et al., 1993) (Beyers et al., 1991) (Halayko and Stelmack 2005).

Disruption of DGC due to the loss of dystrophin leads to DMD; however, abnormal number, size, and shape of caveolae is also evident in DMD, suggesting that dystrophin is not only essential for providing protection against contractile stress, but also the organization of caveolae on the plasma membrane; an incompetent DGC from dystrophin loss leads to the compromise of caveolae compartmentalization (Halayko and Stelmack 2005).

1.6: Overview of Gastrointestinal Tract Structure and Function

The GI tract consists of a series of hollow organs that span from the oral cavity/mouth to the anus, with several accessory organs and glands that add secretions to these hollow organs. Each of these hollow organs are separated by sphincters, which allows these organs to have specialized functions. The mouth and the oropharynx are responsible for the mechanical digestion of dietary substances via mastication (chewing), lubrication of the food, initiation of carbohydrate and lipid digestion via salivary amylase and lingual lipase and propelling the food into the esophagus. The esophagus acts as conduit to the stomach, through which the bolus enters the stomach. The stomach temporarily stores food and initiates mechanical digestion of dietary substances through churning, and chemically digests food through protease and hydrochloric acid (HCl) secretions. Once gastric contents are mixed with the hydrochloric acid and do not exceed a diameter of 2 mm, chyme is orderly transferred to the proximal small intestine (duodenum) through the pyloric sphincter, followed by peristaltic migration distally to the jejunum and then the ileum. The small intestine is the 'hotspot' for nutrient absorption and continues the general digestive processes. Pancreatic enzymes/secretions and brush border enzymes of the small intestine complete digestion by breaking down dietary contents in the correct chemical form that allow for intestinal absorption. Contents of indigestion enter the colon, and travel through the cecum, ascending colon, transverse colon, descending colon, and sigmoidal colon, culminating in the rectum before it has amassed sufficiently to be excreted from the anus.

Accessory organs and glands include the salivary glands, pancreas, and liver. The salivary glands secrete saliva, salivary amylase, and lingual lipase, all of which contribute

to the digestion of carbohydrates and lipids in the oral cavity. The pancreas secretes pancreatic enzymes such as chymotrypsin, amylase, and lipase for the digestion of proteins, carbohydrates, and lipids. In addition, it also secretes bicarbonate (HCO_3^-) to neutralize the incoming gastric acid from the stomach. Bile is produced in the liver and stored in the gallbladder for future delivery in the duodenum for lipid digestion/emulsification.

1.7: Anatomy of Gastrointestinal Wall

The alimentary canal is arranged into certain organizational layers that are common to all segments of the tract. Surrounding the luminal space of the GI tract is the mucosal layer that consists of an epithelial layer, an underlying layer of loose connective tissue called the lamina propria that contains enteric neurons, immune cells, and capillaries, and thin layer of smooth muscle known as the muscularis mucosae. Enclosing the mucosa is the submucosa, a layer of loose connective tissue that contains a larger vasculature than the lamina propria, along with the submucosal plexus (enteric neurons), and glands such as Brunner's glands that secrete substances into the GI lumen. The submucosa is surrounded by the muscularis externa, that consists of an inner circular muscle layer and an outer longitudinal muscle layer. Both are responsible for peristalsis, which is characterized by a progressive wave of relaxation, followed by contraction. The serosa is an enveloping layer of connective tissue lined with mesothelium composed squamous epithelial cells, covering intraperitoneal organs. On the contrary, the adventitia is the outermost connective tissue layer that covers retroperitoneal organs anchored to the posterior abdominal wall.

1.8: Motility Functions of Colon (Large Intestine)

Colonic contractions are regulated by myogenic, neurogenic, and hormonal factors. Parasympathetic control of the proximal two-thirds of the colon is mediated by the vagus nerve, whereas the parasympathetic control of the descending and rectosigmoid colon is mediated via pelvic nerves originating from the sacral spine.

The proximal colon has two types of motor activity, non-propulsive segmentation and mass peristalsis. Non-propulsive segmentation is generated by slow-wave activity that produces circular-muscle contractions that churn and mix the ingesta, presenting them to the mucosa where absorption occurs and moving them in an caudad direction. Antiperistaltic contractions propagate toward the ileum, hampering the movement of the colonic contents through the colon, and allowing further absorption of water and electrolytes. These segmental contractions are what give the large intestine its typical haustra appearance. Haustra are small pouches caused by sacculations, giving the colon its segmented look. The colonic contents during segmental mixing are retained in the proximal large intestine for long periods as fluid and electrolyte absorption continues- giving the large intestine its reservoir function. Mass peristalsis occurs when the colonic contents are propelled distally 20 cm or more, representing the major form of propulsive motility in the colon.

The distal colon is primarily characterized by non-propulsive segmentation. It is in this distal colon that the final desiccation of colonic contents occurs and where these contents are stored prior to an occasional mass peristalsis that propels them into the rectum.

The rectum itself is kept nearly empty by non-propulsive segmentation until it is filled by mass peristalsis of the distal end of the colon. Filling of the rectum triggers a series of reflexes in the internal and external sphincters that ultimately lead to defecation.

1.9: Smooth Muscle Structure with Contractile Protein Emphasis

Smooth muscles are distributed in the walls of various organs and systems, ranging from blood vessels, stomach, intestines, bladder, airways, uterus, and the penile and clitoral cavernosal sinuses (Webb 2003). Smooth muscle cells lack the striated banding pattern found in cardiac and skeletal muscles and receive neural innervation from the autonomic nervous system. The contractile state of the smooth muscle is controlled by hormones, autocrine/paracrine agents, and other local chemical signals. Changes in load or length also develop the tonic and phasic contractions of the SMC's. Regardless of what stimulus regulates the contractile state in SMC's, the cross-bridge cycling between actin and myosin is what ultimately develops force, with Ca^{++} ions initiating contractions (Gunst and Tang 2000).

The contractile apparatus of smooth muscles is very similar to skeletal but is not as highly organized into discrete sarcomeres as in the striated muscles. Thick myosin filaments and thin actin filaments are the primary constituents of the smooth muscle contractile apparatus, colocated in the contractile domain of the cell (Horowitz et al., 1996) (Morgan and Gangopadhyay 2001) (Wang et al., 2012).

Thin filaments are 6-8 nm in diameter and contain actin, which exists as F-actin in vivo, as their main protein constituent. Furthermore, the cellular content of actin in smooth

muscle is ~ twice that of striated muscles. It is well understood that actin-myosin interaction initiates contraction in all three muscle groups; however, there are thin-filament regulatory proteins in smooth muscle that associate with actin and modulate cross-bridge function but are understood at a lesser extent (Babu et al., 2000).

Thick filaments are bipolar assemblies composed of multiple myosin molecules. Each myosin aggregate is composed of two intertwined heavy chains (SM-MHC), a pair of 17-kDa non-phosphorylatable alkali light chains (ELC), and a pair of regulatory 20-kDa light chain (MLC₂₀). The myosin heavy chain dimers form globular amino terminal heads and coiled-coil tails at their carboxy terminus. The myosin head has an intrinsic actin-activated Mg²⁺ ATPase activity, through which myosin is able to transform the chemical energy stored in ATP to mechanical work associated with smooth muscle contraction. Muscle contraction is driven by the cyclical interaction between the myosin thick filament and actin thin filaments coupled with ATP hydrolysis (Farah and Reinach 1995). A cross bridge is formed between the actin and myosin, that produces force and movement as it ‘tilts’ into subsequent bound states until finally detaching (Babu et al., 2000) (Viegas et al., 2003).

1.10: Excitation Contraction Coupling and Thin Filament-Associated Proteins

In all three muscle types, an increase in [Ca⁺⁺]_i triggers contraction via the removal of cross-bridge cycling inhibition (Farah and Reinach 1995) (Holda et al., 1998) (Horowitz et al., 1996) (Merlini et al, 2003). An increase in intracellular Ca⁺⁺ concentrations in the

smooth muscle initiates certain processes that ultimately increase the ATPase activity of myosin. Binding of four Ca^{++} ions to calmodulin forms the Ca^{++} -Calmodulin complex that activates myosin light chain kinase (MLCK), responsible for phosphorylating the regulatory 20-kDa light chain. The principal function of calmodulin in smooth muscle is to activate cross-bridge cycling and development of force in response to the transient increase in intracellular calcium concentration. Rather than troponin C (as in striated muscles), calmodulin is the calcium binding protein responsible for contraction transduction (Farah and Reinach 1995) (Holda et al., 1998) (Horowitz et al., 1996) (Merlini et al, 2003). This phosphorylation of Ser¹⁹ on the 20-kDa regulatory light chain of myosin is fundamental for the actin-activated myosin ATPase and interaction between actin and myosin which initiate smooth muscle contraction (Farah and Reinach 1995) (Holda et al., 1998) (Horowitz et al., 1996) (Kuo and Ehrlich 2015) (Walsh 1994).

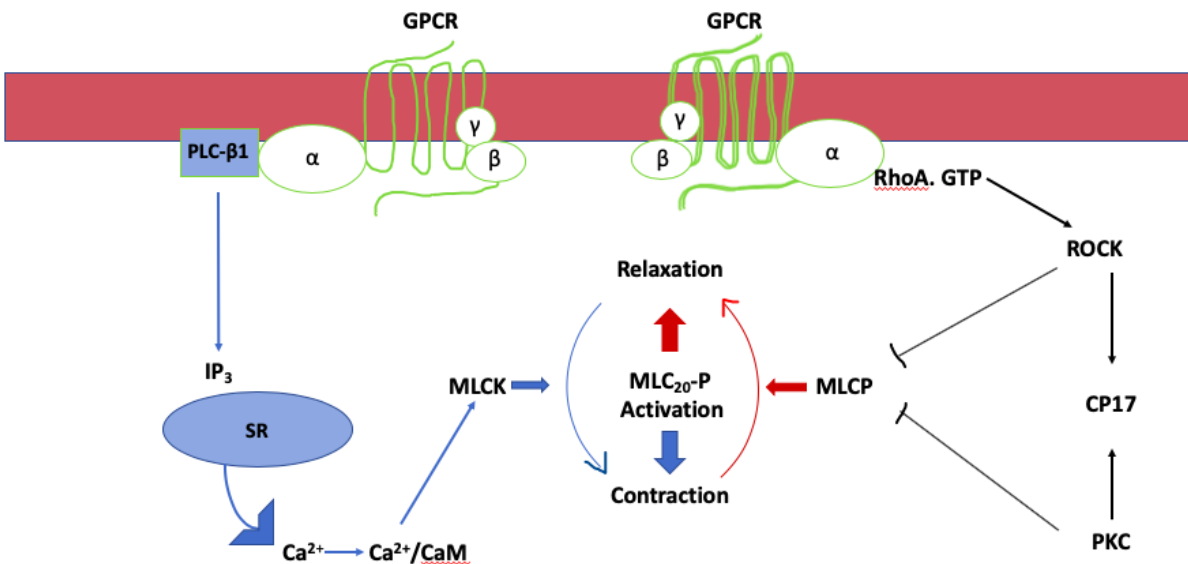


Figure 2. Smooth Muscle Contraction. This figure shows a general summary of the process of smooth muscle contraction. The initial pathway is Ca^{++} and calmodulin (CaM) dependent, where the Ca^{++} /CaM complex activate the myosin light chain kinase (MLCK), triggering contraction via myosin light chain (MLC_{20}) phosphorylation. This represents the initial contraction. The sustained pathway is Ca^{++} /CaM independent and requires the inhibitions of myosin light chain phosphatase (MLCP) to keep the MLC_{20} phosphorylated and the contraction sustained.

GPCR: G-Protein Coupled Receptor; PLC- β 1: Phospholipase C β -1 ; IP₃: Inositol 1,4,5-triphosphate; SR: Sarcoplasmic Reticulum; Ca^{++} : Calcium; CaM: Calmodulin; MLCK: Myosin Light Chain Kinase; MLC_{20} -P: 20 kD Myosin Light Chain; MLCP: Myosin Light Chain Phosphatase; RhoA: Ras Homolog gene family, member A; ROCK: Rho associated, coiled-coil-containing protein kinase 1; CPI17: C-potentiated Inhibitor 17; PKC: Protein Kinase C;

This mechanism pertains specifically to thick filaments, and it is apparent that smooth muscle cross-bridges are regulated by the phosphorylation of MLC_{20} ; however, additional regulation of smooth muscle contraction through thin-filament associated proteins is indicated. Thin-filament regulation is one of several mechanisms invoked to explain the well-known capacity of smooth muscles to maintain tone at low MLC_{20} phosphorylation. These thin-filament associated proteins include: tropomyosin, calponin, caldesmon, and smoothelin (Horowitz et al., 1996) (Morgan and Gangopadhyay 2001).

Tropomyosin. Individual tropomyosin molecules consist of two identical alpha helices that coil around each other and sit near the two grooves that are formed by the two helical actin strands. The head to tail contact between adjacent tropomyosin proteins results in a continuous filament that spans around seven actin monomers (Farah and Reinach 1995)

(Holda et al., 1998) (Horowitz et al., 1996) (Merlini et al, 2003). The role of tropomyosin is to interfere with the binding of myosin to actin. In skeletal muscles, through its interaction with the troponin complex, tropomyosin acts as a Ca^{++} switch turning myosin ATPase activity on and off (Farah and Reinach 1995) (Holda et al., 1998) (Horowitz et al., 1996) (Merlini et al, 2003). In smooth muscles, tropomyosin's role is less clear due to the lack of troponin; however, it is suggested that tropomyosin inhibits acto-myosin ATPase activity in smooth muscle as well, through its interaction with caldesmon^{17,27,33,62}.

Caldesmon. Caldesmon is an actin, tropomyosin, myosin, and calmodulin binding protein. Like the other thin-filament associated proteins, caldesmon also tonically inhibits the ATPase activity of myosin in smooth muscle. It inhibits actin-activated Mg^{2+} -ATPase of smooth muscle myosin by reducing the affinity between actin and myosin. This inhibition is a result of competition between caldesmon and the myosin head for a binding site on actin as both can displace one another from the actin thin filament. Structurally, the carboxy-terminal domains of caldesmon are responsible for actin binding and inhibition of myosin ATPase activity in vitro. The amino-terminal domains bind to myosin and tethers myosin to actin in conjunction with the C-terminal actin binding domains. There are also two high-affinity tropomyosin binding sites on the C-terminal domain of caldesmon and between residues 230 and 419, indicating the function caldesmon plays in tropomyosin-mediated inhibition of acto-myosin ATPase activity. Furthermore, it is observed that the presence of tropomyosin increases caldesmon-actin binding affinity (Farah and Reinach 1995) (Holda et al., 1998) (Horowitz et al., 1996) (Merlini et al, 2003) (Morgan and Gangopadhyay 2001).

Calponin. Calponin is another thin-filament associated protein that like caldesmon, tonically inhibits the interaction between myosin and actin. Its function of binding to F-actin and inhibition of ATPase activity are localized to its central domain. Calponin inhibits the ATPase activity of myosin heads cross-linked to actin resulting from a conformational change in actin induced by calponin binding and actin's reduced capacity to activate myosin ATPase. It contains three isoforms, h1, h2, and an acidic variant, with h1 being smooth muscle specific (Holda et al., 1998) (Horowitz et al., 1996) (Merlini et al, 2003) (Morgan and Gangopadhyay 2001).

Smoothelin. Smoothelin's are actin-binding proteins that are abundantly expressed in visceral smooth muscle as smoothelin-A, and expressed in vascular smooth muscle as smoothelin-B⁴⁷. Both isoforms of smoothelin are found only in actively contracting smooth muscles. During pathological conditions associated with GI tract or vascular system, smoothelin-A and smoothelin-B expression is lower with adverse effects being apparent in the contractility of the two systems. Ultimately, it is understood that smoothelin is imperative for optimal contractility of smooth muscle, but the mechanism through which it accomplishes its function is not clear (Niessan et al., 2005).

1.11: Excitation-Transcription Coupling

Excitation-transcription coupling is a process that is highly dependent on $[Ca^{++}]_i$ – specific stimuli and activates various transcription factors that elicit transcriptional responses depending on the conditions of the cell both extracellularly and intracellularly⁴². Smooth muscle cells of the vascular system require expression of a unique range of

contractile proteins/genes like SM-MHC, SM22alpha, calponin, smoothelin, etc (Misarkova et al., 2016) (Wamhoff et al., 2006).

CREB (cAMP response element binding protein). CREB is highly expressed and active in quiescent smooth-muscle cells. It promotes smooth muscle gene expression and decreases proliferation through regulating the expression of cell cycle regulatory genes, genes encoding for growth factors, growth factor receptors, and cytokines. cAMP/PKA pathway, MAPK pathway, and more importantly the Ca^{++} - Calmodulin complex, which activates MLCK and promotes MLC_{20} phosphorylation to induce contraction, also promotes the phosphorylation of CREB via CamK regulation (Wamhoff et al., 2006) (Marchand et al., 2012).

NFAT and NFkB. NFAT transcription factors include 4 isoforms, NFAT1, NFAT2, NFAT3, and NFAT4. These factors are activated by calcineurin, a Ca^{++} - Calmodulin-dependent phosphatase that is activated during EC/ET- coupling by myofibril Ca^{++} fluctuations. The dephosphorylation of NFAT by calcineurin allows for its translocation to the nucleus, where expression of SM-MHC and actin are increases, suggesting its role in regulating expression of different SMC marker genes (Marchand et al., 2012).

Ca^{++} /CArG element. Expression of the majority of SMC markers genes like actin, SM-MHC, SM22a, and h1 calponin have been shown to be dependent on at least one CArG element, located in the promoter-enhancer regions of these genes, and intracellular Ca^{++} concentration. During depolarization-induced calcium influx through the L-type voltage-gated Ca^{++} channels, there's an increase in the mRNA levels of actin, SM-MHC, and

SM22a. The L-type voltage-gated Ca^{++} channels activation was CARG dependent (Marchand et al., 2012).

1.12: Muscular Dystrophy- Abnormal Gastrointestinal Motility

Various clinical manifestations such as bloating, fullness, slow colonic transit, and chronic constipation have been reported in the gastrointestinal tract, often with life-threatening complications. Despite postmortem evidence of significant gastro-intestinal smooth muscle degeneration in DMD, its mechanism, GI function, and treatment have not yet been systematically studied (Lo Cascio et al., 2016) (Mule et al., 2010). It has been speculated that reduced slow-wave activity, along with the reduced availability of intestinal NO (due to the lack of dystrophin) might be a possible mechanism for the reduced intestinal motility and transit time (Lo Cascio et al., 2016) (Mule et al., 2010). Furthermore, this lack of dystrophin causes the linkage between the cytoskeleton and extracellular matrix to break, making muscles more susceptible to contraction-induced damage. This damage is associated with plasma membrane tears and ruptures, causing Ca^{++} influx and intracellular overload of Ca^{++} . There are morphological signs of significant reduction in the thickness of the muscular layer, mucosal degeneration and damage to the internal membrane of mitochondria in the large intestine of DMD mice. Nonetheless, the cause of this damage and reduced contractility is not fully understood (Alves et al., 2014) (Ryder et al., 2014) (Sarna et al., 2010).

1.13: Oxidative Stress

Oxidative stress and inflammation are proposed pathogenic mechanisms that can explain the dystrophic pathophysiology. Smooth muscles lacking functional dystrophin have an increased susceptibility to sarcolemmal damage after muscle contraction, leading to necrosis and oxidative stress, where this stress seems to exacerbate the pathology of DMD. The precise understanding of why this dystrophin deficiency causes ROS production is not clear; however, it is likely correlated with the excessive amounts of intracellular Ca^{++} coupled with inflammation (Chahbouni et al., 2010).

Elevated cytosolic Ca^{++} levels lead to an increase in mitochondrial Ca^{++} , which is an effector of ATP synthesis. An increase in ATP synthesis causes an increase in the ROS production by the mitochondria through higher O_2 consumption and enhanced e^- flow through the electron transport chain (Terril et al., 2013). Membrane damage, due to the contraction-induced damage in dystrophin deficient smooth muscles, results in the degranulation of mast cells and release of intracellular contents, activating the immune system. Immune cells like neutrophils and macrophages generate ROS in order to promote phagocytosis. NF κ B immunoreactivity has also been detected in the plasma, macrophages and necrotic and non-necrotic fibers in the muscle of DMD patients. The NF κ B transcription factor plays a role in the expression of TNF α and IL-1 β , which in turn stimulate further production of ROS (Chahbouni et al., 2010) (Singh and Lin 2015).

1.14: Hydrogen Sulfide (H_2S) – Physiological Effects

Smooth muscle relaxation. Hydrogen Sulfide is well-known as a poisoning and toxic pollutant. However, just like nitric oxide NO and carbon monoxide CO, it is

considered a gasotransmitter that induces relaxation in the smooth muscles (Mancardi et al 2009). H₂S is produced both enzymatically and non-enzymatically in the GI tract. The enzymes, cystathionine-B- lyase (CBS) and cystathionine-γ-lyase (CSE), are found in the GI tract of mice, rat, and the colon of healthy humans. These enzymes are able to produce H₂S via the reduction of cysteine. Non-enzymatic production of H₂S in the GI tract is associated with sulfur reducing bacteria present in the large intestine (Wang 2012).

The best-known physiological role for NO is as an endothelial-derived relaxing factor (EDRF) which shows vasorelaxant actions. H₂S, like NO, has been shown to induce smooth muscle relaxation in the blood vessels as seen with hypertension development in mice with CSE knocked out (Kimura, 2011). Relaxation of these smooth muscles occurs mostly via the opening of ATP-dependent K⁺ channels⁵⁸. This process of causing vasodilation of through the opening of ATP-dependent K⁺ channels preconditions against ischemia/reperfusion injury and myocardial infarction. A multitude of findings support this concept: K⁺-dependent ATP channel blockers attenuated H₂S induced vasodilation both in vivo and in vitro. The relaxing effect of H₂S on colonic motility has also been explained, in part, by its direct inhibition of the L-type C⁺⁺ channels. An endothelium-dependent effect is also seen to contribute to these vasodilatory properties. In human endothelial cells, H₂S caused direct inhibition of the angiotensin-converting enzyme and enhanced the vasorelaxation induced by NO (Kimura, 2011) (Singh and Lin 2015)

Antioxidation. H₂S also consists of a thiol group that allows it to reduce disulfide bonds and carry out biological effects as an antioxidant. In neurodegenerative diseases, like Alzheimer's, H₂S exerts its antioxidant function as a peroxynitrite scavenger. In the brain's

of Alzheimer patients, considerably low levels of H₂S are noted with protein nitration by peroxynitrite increased. When testing the effects of the ‘H₂S’ donor NaSH (sodium hydrogen sulfide) in cultured human SH-SY5Y cells, H₂S significantly inhibited peroxynitrite-mediated tyrosine nitration, peroxynitrite-induced cytotoxicity, intracellular protein nitration and protein oxidation (Whiteman et al., 2004).

Another H₂S donor/prodrug, SG1002, was used to investigate its effects on stress induced hypertrophic signaling in murine HL1 cardiomyocytes. SG1002 increased levels of H₂S producing enzyme, CBS, as well as significantly inhibiting H₂O₂ and ET-1/Phe induced oxidative stress (Whiteman et al., 2004).

Treatments. It is understood that dystrophin loss predisposes all muscle fiber types to contraction-induced damage that ultimately leads to muscle degeneration (Lim et al., 2017). Today, treatment for DMD uses a multidisciplinary approach as multiple organ systems are affected, and these treatments are palliative at best- hoping to manage the complications with ambulation, respiration, and cardiac health in DMD patients. Prolonged, high-dose corticosteroid treatment has been most widely utilized due its effectiveness in delaying the disease progression by specifically affecting the aspect of muscle wasting presented in DMD (Biggar et al., 2001). Steroidal drugs such as prednisone and deflazacort have shown to preserve muscle function, with increasing muscle mass and slowing muscular degradation. However, the therapeutic benefits of corticosteroid treatment are temporary, with disease progression only being delayed and various adverse side effects such as growth retardation, weight gain, hypertension, and cataracts developing (Hori et al., 2011) (Merlini et al 2003)

Now, as aforementioned, oxidative stress is an important downstream signal in the dystrophin process, particularly due to the dysregulation of intracellular Ca⁺⁺ homeostasis caused by contraction-induced damage and mitochondrial damage. The existence of this hyper oxidative status in the DMD phenotype not only implicates the role of ROS in the pathophysiology of DMD, but also the importance of antioxidant therapeutics for DMD treatment. Recently, antioxidants such as resveratrol and melatonin have been used for DMD treatment in *mdx* mice, and they presented a reduction in ROS levels, fibrosis, cardiac dysfunction, and an increase in lifespan (Biggar et al 2001) (Hori et al 2011) (Chahbouni et al 2010).

1.15: Mouse Models of DMD

Knowledge of how lack of the gene for the cytoskeleton protein dystrophin leads to DMD has led to the development of various mouse models used for DMD research.

There are both naturally occurring and laboratory-generated animal models that are used to study the pathophysiology of DMD and therapeutic efficacy of drugs on the disease. Currently, there are around 60 different mouse models for DMD (Mcgreevy et al., 2015).

The standard model of DMD is the *mdx* mouse, which carries the mutated dystrophin gene that is found in DMD patients. However, despite this deficiency in dystrophin, *mdx* mice lack the severe clinical manifestations that are present in DMD patients- the lifespan is only reduced by ~25% in *mdx* mice compared to the ~75% reduction seen in DMD patients. There is also a well-known discrepancy in the muscular

wasting that is displayed in DMD patients compared to the *mdx* mouse (Mcgreevy et al., 2015) (Fulmer 2011).

There are, however, mice models available that overcome this discrepancy, displaying a more severe phenotype of the DMD disease. Studies have shown that muscle cells of DMD patients have reduced proliferative and regenerative potential than muscles of healthy subjects' due to telomerase shortening. In mice, there is minimal telomerase shortening with age progression, which is implicated as a cause for the discrepancy seen between *mdx* mice and DMD patients in regard to muscle degradation. Consequently, the *mdx/mTR* *-/-* mouse model was created, which is a double knockout (KO) mouse that lacks not only dystrophin, but also the telomerase RNA component (*Terc*) that maintains chromosome telomere length. Other major DMD mouse models include: utrophin KO mouse (*mdx/Utrn* *-/-*), α -dystrobrevin KO mouse (*mdx/Dtna* *-/-*), α -7 integrin KO mouse (*mdx/ α -7* *-/-*), and Myod1 deficient mice (*mdx/Myod1* *-/-*) (Fulmer 2011) (Mourkioti et al 2013).

1.16: Rationale

The clinical effects of DMD in the large intestine of the gastrointestinal tract are commonly seen in DMD affected patients and animal models yet information on the mechanism and treatment of these complications have not been evaluated. Most of the underlying cause of aberrant GI function is correlated with hypocontractility; however, the cause of this hypocontractility in DMD patients and the effect that dystrophin deficiency has on contractile protein expression in smooth muscle are unknown. H₂S is a well-known

gasotransmitter that promotes gut motility and regulates the expression of contractile proteins by its signaling pathway as an inhibitory transmitter. Nonetheless, its effect on colonic motility in DMD is unknown.

Hypothesis. My aim is to investigate the effect the DMD phenotype has on the levels of thin-filament associated proteins and colonic smooth muscle contractility. I hypothesize that the lack of dystrophin will lead to a decrease in contractile protein mRNA expression and smooth-muscle function. Furthermore, oxidative stress is considered an important process in the pathophysiology of DMD, thus, my aim is to also examine whether H₂S, which is known to have antioxidant function, can restore the effects of dystrophin deficiency. I hypothesize that H₂S treatment restores the effects of dystrophin deficiency.

Approach. Contraction and relaxation of colonic segments were measured in their longitudinal orientation from 3-month-old control and *mdx* mice, and 9-month-old control and *mdx/mTR* mice using organ bath systems. The effect of the H₂S prodrug, SG1002, was tested in *mdx/mTR* mice. The expression of contractile proteins in *mdx* and *mdx/mTR* mice along with their age-matched control was measured using qRT-PCR and Western Blotting.

Chapter 2: MATERIALS AND METHODS

2.1 : Reagents

Antibodies for Calponin, Caldesmon, and Smoothelin were obtained from Abcam (Cambridge, MA). Antibody for Tropomyosin was obtained from Santa Cruz Biotechnologies, Inc. (Dallas, TX); GAPDH was obtained from Cell Signaling Technology (Danvers, MA) RNAqueous™ kit, TRIzol Reagent, High-capacity cDNA Reverse Transcription Kit, PCR Primers for Calponin (Cnn1 Mm00487032-m1 59 bp), Caldesmon (Cald1Mm00513995-m1 102 bp), Tropomyosin (Tpm2 Mm00437172-g1 97 bp), Smoothelin (Smtn Mm00449973 m1 66 bp), GAPDH (NM-008084.2 107 bp), β -actin (Actb Mm02619580-g1), and 18-S (4332641) were obtained from Thermo Fisher (Waltham, MA); Western Blotting materials, 2x Laemmli Sample Buffer, DC™ Protein Assay Reagents, Clarity Max Western ECL Substrate, Clarity Western ECL were obtained from Bio-Rad Laboratories (Hercules, CA) T-PER® Tissue Protein Extraction Reagent was obtained from Thermo Scientific (Rockford, IL). All other supplies from Sigma, (St.Louis, MO); and Fisher Scientific, (Asheville, NC).

2.2 : Animals

3-month-old female wild-type (WT) and *mdx* mice (C57BL/6) were purchased from Jackson Laboratory (Sacramento, California). The mice were housed in an animal facility directed by the Division of Animal Resources at VCU. 9-month-old male WT, *mdx/mTR*, and *mdx/mTR* treated mice were received from Dr. Salloum's lab at Sanger Hall, who

purchased their mice from the Jackson Laboratory (Sacramento, California). All procedures were approved by the Institutional Animal Care and Use Committee (IACUC) of the Virginia Commonwealth University.

2.3: H₂S Treatment

mdx/mTR mice in Dr. Salloum's lab were treated with the H₂S prodrug, SG1002, at different time intervals, creating two different treatment cohorts of mice. SG1002, the orally active slow-releasing H₂S prodrug, was administered as 40 mg/kg of body weight in chow/every 3 days in *mdx/mTR* mice: Early treated mice were given SG1002 from 21 days old to 12 months, and late treated mice were given SG1002 from 7 months to 12 months old.

2.4: Collection of Tissue/Preparation of Colonic Tissue

Mice were euthanized by CO₂ inhalation and carefully observed for signs of complete cessation. Vertical incisions on the abdomen of the mouse model were performed, and the colon was removed and placed in smooth muscle buffer (SMB), 1X phosphate-buffered saline (PBS), or Krebs buffer solution, depending on the experimental method being performed. Luminal contents of the colonic tubes were appropriately flushed with a blunt syringe filled with SMB, PBS, or Krebs buffer. The colonic tubes were cut opened along the meso-colon with surgical ring scissors. The mucosa was carefully scraped from the smooth muscle layer, containing enteric neurons and smooth muscle cells (SMC's) via round edged forceps.

For RNA isolation and lysate preparation, tissues were cut on ice and kept 'hydrated' with PBS. For smooth muscle cell isolation, tissues were placed in SMB [NaCl 120 mM, KCl 4 mM, KH₂PO₄ 2.6 mM, CaCl₂ 2.0 mM, MgCl₂ 0.6 mM, HEPES (N-2-hydroxyethylpiperazine-N' 2-ethanesulfonic acid) 25 mM, glucose 14 mM, and Basic Eagle Medium (essential amino mixture) 2.1% (pH 7.4)]. For organ bath studies, Segments of colon, approximately 1 cm long, were immediately collected/removed and lacerated along the long axis of the mesenteric border. The mucosa was abraded carefully. The resulting longitudinal segments of colon tissue were pinned in a flat petri dish containing warm (37°C), oxygenated Krebs buffer solution [118 mM NaCl, 4.8 mM KCl, 1 mM MgSO₄, 1.15 mM NaH₂PO₄, 15 mM NaHCO₃, 10.5 mM glucose and 2.5 mM CaCl₂ (95% O₂/5% CO₂, pH 7.4, 37°C).

2.5 : Preparation of Dispersed Smooth Muscle Cells

Smooth muscle cells were isolated from the colon by sequential enzymatic digestion, filtration, and centrifugation. Colonic tissue, carefully removed of the mucosa and chopped via surgical shears as aforementioned, was incubated at 31°C for 10-15 minutes in SMB containing 0.1 % collagenase and 0.01% of soybean trypsin inhibitor. The partially degraded tissue was washed once with collagenase-free SMB and permitted to disperse spontaneously for 20 minutes. Cells were then collected/harvested through a 500 um Nitex every 10 minutes.

2.6: Measurement of Contraction in Muscle Strips

The isolated smooth muscle strips were tied at the proximal and distal end by silk thread using caution as to not restrict the luminal portion. Each colonic segment was longitudinally mounted between a glass rod and isometric force transducer and submerged in an organ bath. Each organ bath was filled with either 7ml or 3.5 ml of Kreb's (depending on the size of the organ bath) and bubbled continuously with 95% O₂ and 5% CO₂ at 37°C to maintain constant temperature in the bath systems. All the strips were raised to 0.7-0.8 grams of tension and allowed to equilibrate for 1 hour, with flushing and refilling organ baths with Krebs solution every 15 minutes. Contraction was induced via muscarinic receptor activation (acetylcholine) at a concentration of 10 μM of acetylcholine (ACh). Relaxation was measured in response to 10 μM of sodium-nitroprusside (SNP), a NO donor that induces relaxation. The contractile response of the colonic segments to muscarinic receptor activation was measured in grams and expressed as mN/100 mg of tissue by multiplying grams by 9.8 mN. At the end of each experiment, the strips were blotted dry and weighed (tissue wet weight). The mean tissue weight of 3-month-old control mice was 10.66±1.53 and the mean tissue weight of 3-month-old *mdx* mice was 10.75±1.38.

2.7: Measurement of Contraction in Dispersed Smooth Muscle Cells

Contraction in freshly dispersed colonic muscle cells was determined by scanning micrometry. A cell aliquot consisting of 10⁴ cells/ml was treated with 500 μl of medium containing acetylcholine (ACh, 10 μM) for 30 s or 5 minutes and the reaction was

terminated with 1% acrolein at a final concentration of 0.1%. Acrolein, which kills and fixes cells without affecting the cell length. The resting cell length was determined in control experiments in which muscle cells were incubated with 500 μ l of 0.1% bovine serum albumin without the ACh. The mean lengths of 50 muscle cells treated with acetylcholine was measured by scanning micrometry and compared with the mean lengths of untreated cells. The contractile response was expressed as the percent decrease in mean cell length from control cell length.

Relaxation was measured in intact muscle cells contracted with ACh (1 μ M). Muscle cells were treated for 5 minutes with isoproterenol (10 μ M) followed by ACh for 30 s or 5 min. The reaction was terminated with 1% acrolein. The length of 50 cells treated with acetylcholine was measured in sequential microscopic fields by scanning micrometry. Relaxation was expressed as percent increase in the length of cells contracted with ACh.

2.8: Qualitative Real-Time PCR Analysis (qRT-PCR)

To obtain mRNA from colonic tissue, 1 mL of TRIzol reagent was added to ~40-100 mg of tissue. The mixture was homogenized via Fisher PowerGen 125 homogenizer. 200 μ L of chloroform was added to separate the solution in an aqueous and organic phase. The RNA remained in the aqueous phase. The solution is vortexed and allowed to incubate at room temperature for 5 minutes, then centrifuged at 13.3 rpm at 4°C for 15 minutes. The superior aqueous phase was transferred to a new autoclaved eppendorf tube and 0.5 ml of isopropanol was added to dissolve any salts that may have chelated on the RNA samples. The solution is vortexed and centrifuged at 13.3 rpm at 4°C for 20 minutes. The resulting

supernatant is then discarded, and 1 ml of ethanol is added, allowing precipitation of RNA out of the aqueous solution. The mixture is centrifuged at 13.3 rpm at 4°C for 10 minutes. The ethanol was then removed, and the eppendorf tubes are vacuum dried until all liquid phase contents have been evaporated. Twenty-five microliter of RNase and DNase free ultrapure distilled water is added and the tubes are allowed to incubate at 65°C for 10 minutes. Concentration was measured using Nanodrop8000.

RNA from each preparation was reversely transcribed using the High Capacity cDNA reverse transcription kits to prepare the 2x RT Master Mix [10x RT Buffer, 25x dNTP Mix, 10x RT Random primers, Multiscribe Reverse Transcriptase, Nuclease Free H₂]. An equal volume of RNA was added to 2xRT Master Mix. Quantitative RT-PCR was then performed on cDNA samples using the specific primers of: Tropomyosin, Caldesmon, Calponin, and Smoothelin, based on known sequences in mouse and Taqman gene expression master mix. 18-S and β -actin expression were used as controls to normalize expression of the target genes. The primers were designed to satisfy the use of $2^{-\Delta\Delta CT}$ method, which is the standard method of comparing gene expression between two groups. With 18-S/ β -actin acting as controls, a quantitative comparison between *mdx*, *mdx/mTR* and their age-matched control was calculated using the $2^{-\Delta\Delta CT}$ method. Final calculations were expressed as a fold difference in the expression of *mdx*, *mdx/mTR*, and treated *mdx/mTR* mice cohorts relative to their age-matched control.

2.9: Western Blot Analysis

Colonic tissue, not exceeding 50 mg, were taken from animal models, cleaned and removed of the mucosa (as aforementioned), and transferred into new eppendorf tubes with appropriate amounts of 1.44mm beads and TPER (lysis buffer) in the presence of protease inhibitor. Bead number was calculated as 5 times the tissue weight with TPER volume being double the tissue weight. Tissues were homogenized using a bullet blender. The supernatant was collected and centrifuged at 13.3 rpm at 4°C for 10 minutes. Protein concentration was then measured using a DC protein assay kit from Bio-Rad. Equal amounts of proteins were fractionated by SDS/PAGE and transferred on to Polyvinylidene difluoride (PVDF) membrane. Blots were blocked with 1X TBS with 1% casein blocker for 1 hour at room temperature and then incubated overnight at 4 °C with various primary antibodies in 1X TBS with 1% casein (Calponin 1:5000, Tropomyosin 1:1000, Caldesmon 1:10,000, Smoothelin 1:5000). After incubation for 1 h with horseradish-peroxidase-conjugated corresponding secondary antibody (1:5000) in 1X TBS with 1% casein, immunoreactive proteins were visualized using Clarity Max Western ECL Substrate, Clarity Western ECL Substrate, or SuperSignal West Pico Chemiluminescent Substrate kit. All washing steps were performed with TBS-T. The protein bands were identified by enhanced chemiluminescence reagent.

3.0: Statistical Analysis

Data and results are presented as means \pm Standard Error Mean (SEM). All experiments were completed four or more times. Results were analyzed for statistical significance using unpaired student T tests. p values < 0.05 were considered significant.

Chapter 3: RESULTS

3.1 Effect of DMD on Smooth Muscle Contraction and Relaxation

To assess the role of what dystrophin loss has on colonic smooth muscle function, we utilized *mdx* and *mdx/mTR* mouse models of that lack dystrophin and express the DMD phenotype. Effect of H₂S treatment on the smooth muscle contractile function in the *mdx/mTR* mouse model was assessed. Colonic tissue from *mdx/mTR* mice treated with SG1002, an orally active slow-releasing compound that provides stable, non-toxic serum and tissue levels of H₂S. SG1002 is seen to induce cardioprotection in murine models of DMD; however, its therapeutic potential in the GI tract of DMD mice has not been evaluated. Colonic tissue from *mdx/mTR* mice and *mdx/mTR* mice treated with SG1002 were kindly provided by Dr. Salloum. Smooth muscle function was measured as contraction in response to acetylcholine (activator of the main excitatory muscarinic receptor pathway), and relaxation in response to sodium nitroprusside, nitric oxide (NO) donor (activator of the main inhibitory nitrenergic pathway) and isoproterenol (activator of inhibitory β -adrenergic pathway). Contraction and relaxation were measured in intact colonic muscle segments and isolated colonic muscle cells.

Contraction and relaxation in muscle strips. For isometric contractions, intact colonic segments from *mdx* mice, *mdx/mTR* mice, and their age matched control were placed longitudinally in an organ bath with Krebs buffer. Acetylcholine (ACh, 10 μ M) was administered to induce contraction in the colonic tissues. Force of contraction was measured in grams. In muscle segments from control mice acetylcholine typically

produced 0.7 ± 0.2 g of contraction and the contraction was inhibited (0.3 ± 0.1 g) in muscle segments from *mdx* mice (Figure 3, left panel). Contraction in grams was normalized to tissue and presented as mN/100 mg tissue. ACh-induced contractions in colonic muscle segments from *mdx* mice was significantly lower compared to their age-matched control (15.6 ± 3.9 mN/100 mg tissue in control and 3.8 ± 1.4 mN/100 mg tissue in *mdx* mice; $p < 0.05$, $n = 4-5$) (Figure 3, right panel).

ACh-induced contraction was also significantly decreased in colonic segments from *mdx/mTR* mice compared to their age-matched control (12.4 ± 2.3 mN/100 mg tissue in control and 4.2 ± 1.3 mN/100 mg tissue in *mdx/mTR* mice; $p < 0.05$, $n = 4$) (Figure 4). Although, *mdx/mTR* mice are shown to exhibit much severe phenotype of DMD, inhibition of contraction in colonic muscle strips from *mdx* mice is observed to be slightly greater than the inhibition in colonic segments *mdx/mTR* mice ($73 \pm 6\%$ inhibition in *mdx* mice versus $65 \pm 6\%$ inhibition in *mdx/mTR* mice).

Isometric contractions of colonic segments from *mdx/mTR* mice treated with SG1002 were also evaluated. Acetylcholine-induced contraction in colonic segments from *mdx/mTR* mice treated with SG1002 was significantly improved compared to colonic segments from *mdx/mTR* mice (9.2 ± 1.4 mN/100 mg in *mdx/mTR* mice treated with SG1002 versus 4.2 ± 1.3 in *mdx/mTR* mice) (Figure 4). The inhibition of contraction in *mdx/mTR* mice treated with SG1002 was significantly less compared to *mdx/mTR* mice ($23 \pm 5\%$ inhibition versus $65 \pm 6\%$ in *mdx/mTR* mice. $p < 0.01$, $n = 4$). These results suggest that H₂S reversed the decrease in smooth muscle contraction in *mdx/mTR* mice and restored closer to normal levels.

Relaxation in response to SNP in muscle strips was measured as inhibition of ACh-induced contraction. Muscle strips were treated with ACh (10 μ M) and after attaining a stable contraction, SNP (10 μ M) was added to measure relaxation. SNP induced complete relaxation of ACh-induced contraction in muscle strips from control, *mdx* and *mdx/mTR* mice. There was no significant difference in relaxation in response to SNP between *mdx* mice and their age matched control (96 \pm 2% in control and 94 \pm 3% in *mdx* mice) and *mdx/mTR* mice, *mdx/mTR* mice (treated with SG1002) and their age-matched control (125 \pm 5% in control mice, 105 \pm 10 in *mdx/mTR* mice and 108 \pm 7% in *mdx/mTR* mice treated with SG1002) (Figures 5 and 6). These results suggest that relaxation in response to NO donor was not affected in colonic muscle of *mdx* and *mdx/mTR* mice.

Contraction and relaxation in isolated muscle cells. Contraction and relaxation in response to acetylcholine and SNP in innervated muscle strips could be accredited to the release of transmitters from enteric neurons and/or to the effect of interstitial cells of Cajal (ICC) that modulate the intrinsic electrical and mechanical activity of smooth muscles. To identify the specific involvement of smooth muscle dysfunction to the muscle itself, colonic muscle cells devoid of enteric neurons and ICC were isolated from *mdx* mice and their age-matched controls, and contraction in response to ACh was measured and expressed as the percent decrease in basal cell length. The kinetic of acetylcholine-induced contraction consists of an initial Ca⁺⁺-dependent phase involving activation of Ca⁺⁺/calmodulin-dependent MLC kinase and increase in MLC₂₀ phosphorylation and a

Ca⁺⁺-independent phase involving inhibition of MLC phosphatase and increase in MLC20 phosphorylation. We measured both initial and sustained contraction in response to ACh in isolated muscle cells.

The basal cell lengths of colonic smooth muscle cells were not significantly different in control mice and *mdx* mice (68±4 μm in control mice and 64±6 μm in *mdx* mice). Treatment of cells with ACh for 0.5 min (initial contraction) caused a significant decrease in muscle cell length both in the colon of control and *mdx* mice. However, the contraction in response to ACh was significantly inhibited in muscle cells from colon of *mdx* mice compared to control mice (43±5% decrease in cell length in control mice and 25±3% decrease in muscle cell length in *mdx* mice; p<0.05, n=4-5) (Figure 7). Treatment of cells with ACh for 5 min (sustained contraction) caused a significant decrease in muscle cell length both in the colon of control and *mdx* mice. However, the contraction in response to ACh was significantly inhibited in muscle cells from colon of *mdx* mice compared to control mice (40±4% in control and 27±3 in *mdx* mice; p<0.05, n=4-5) (Figure 8). The results in isolated muscle cells are consistent with the results in muscle strips and suggest that inhibition of contraction in colonic muscle strips is due to a defect in the mechanisms that regulate contraction intrinsic to smooth muscle cells.

In colonic smooth muscle, inhibitory transmitters that activate cAMP/PKA or cGMP/PKG pathway cause muscle relaxation. To examine whether the pathways that mediate relaxation was affected in *mdx* mice, relaxation was also measured in isolated smooth muscle cells from the colon of control and *mdx* mice. To measure relaxation, muscle cells were pretreated with SNP (10 μM) or isoproterenol (10 μM) and contraction

in response to ACh (1 μ M) was measured. Decrease in ACh-induced contraction in the presence of SNP or isoproterenol reflects muscle relaxation and it was expressed as percent inhibition of contraction (i.e., relaxation). Relaxation in response to SNP was not significantly different in muscle cells isolated from the colon of control and *mdx* mice. SNP caused $83\pm 12\%$ relaxation in muscle cells from control mice and $92\pm 6\%$ relaxation in muscle cells from *mdx* mice. (Figure 9). These results suggest that NO-dependent relaxation mediated via cGMP/PKG pathway was not different in colonic muscle cells from control versus *mdx* mice. Isoproterenol also caused $79\pm 6\%$ relaxation in muscle cells from control mice and $77\pm 5\%$ relaxation in muscle cells from *mdx* mice. (Figure 10). These results suggest that G protein-coupled receptor-dependent relaxation mediated via cAMP/PKA pathway was not different in colonic muscle cells from control versus *mdx* mice. The results in isolated muscle cells are consistent with the results in muscle strips and suggests that intrinsic relaxation mechanisms mediated by cAMP/PKA and cGMP/PKG pathway are not altered in *mdx* mice.

3.2 Changes in the Expression of Thin Filament-Associated Proteins

In smooth muscle contraction is mediated by interaction of actin with myosin. However, this interaction is modulated by thin filament associated proteins. In the present study, we also analyzed the changes in expression of the thin filament-associated proteins caldesmon, calponin, tropomyosin, and smoothelin by qRT-PCR and western blot in smooth muscle of colon isolated from *mdx*, *mdx/mTR*, and their age-matched control mice.

Caldesmon. Caldesmon is a thin-filament associated protein that regulates smooth muscle contraction via its interaction with actin. Caldesmon has two isoforms, h-caldesmon that is smooth muscle specific and l-caldesmon that is a non-muscle isoform (Morgan KG, 2001). Expression of caldesmon mRNA was measured using primers specific for smooth muscle isoform by qRT-PCR in colonic smooth muscle from control and *mdx* mice and expressed as fold change from control levels. Expression of caldesmon mRNA was significantly decreased in colonic smooth muscle from *mdx* mice compared to control levels ($p < 0.05$, $n=4-5$) (Figure 11 Left Panel). Expression of caldesmon protein was measured using antibodies that are not specific to smooth muscle isoform. Western blot analysis showed no changes in the expression of caldesmon in colonic smooth muscle between control and *mdx* mice (Figure 11 Right Panel).

Expression of caldesmon mRNA was also significantly decreased in *mdx/mTR* mice compared to control levels and the decrease in expression was partly reversed by treatment of *mdx/mTR* mice with SG1002 (Figure 12). The effect of SG1002 on caldesmon mRNA expression was significant ($p < 0.05$, $n=4$).

Calponin: Calponin is another thin filament-associated protein that exists in three isoforms, h1-acidic, h2-neutral, and basic calponin. The h1-acidic isoform is smooth-muscle specific, whereas the other two are non-muscle isoforms. Expression of calponin mRNA was measured using primers specific for smooth muscle isoform by qRT-PCR in colonic smooth muscle from control and *mdx* mice and expressed as fold change from control levels. Expression of calponin mRNA was significantly decreased in colonic smooth muscle from *mdx* mice compared to control levels ($p < 0.05$, $n=4-5$) (Figure 13 Left

Panel). Expression of calponin protein was measured using antibodies that are not specific to smooth muscle isoform. Western blot analysis showed no changes in the expression of calponin in colonic smooth muscle between control and *mdx* mice (Figure 13 Right Panel).

Expression of calponin mRNA was also significantly decreased in *mdx/mTR* mice compared to control levels and the decrease in expression was completely reversed by treatment of *mdx/mTR* mice with SG1002 (Figure 14). The effect of SG1002 on calponin mRNA expression was significant ($p < 0.05$, $n = 4$).

Tropomyosin: Tropomyosin, like calponin and caldesmon, is a thin filament-associated protein that regulates acto-myosin interaction. Two isoforms of tropomyosin exist, α and β tropomyosin. Expression of tropomyosin mRNA was measured using primers that are not isoform-specific by qRT-PCR in colonic smooth muscle from control and *mdx* mice and expressed as fold change from control levels. Expression of tropomyosin mRNA was significantly decreased in colonic smooth muscle from *mdx* mice compared to control levels ($p < 0.05$, $n = 4-5$) (Figure 15 Left Panel). Expression of the tropomyosin protein was measured using antibodies that are not isoform-specific. Western blot analysis showed no changes in the expression of tropomyosin in colonic smooth muscle between control and *mdx* mice (Figure 15 Right Panel).

Smoothelin: There are two isoforms of smoothelin, smoothelin-A that is specific to the visceral smooth muscle and smoothelin-B that is specific to vascular smooth muscle. Expression of smoothelin-A mRNA was measured using primers that are specific for visceral smooth muscle by qRT-PCR in colonic smooth muscle from control and *mdx* mice and expressed as fold change from control levels. Expression of smoothelin-A mRNA was

significantly decreased in colonic smooth muscle from *mdx* mice compared to control levels ($p < 0.05$, $n=4-5$) (Figure 16 Left Panel). Expression of smoothelin protein was measured using antibodies that are not isoform-specific. Western blot analysis showed no changes in the expression of smoothelin in colonic smooth muscle between control and *mdx* mice (Figure 16 Right Panel).

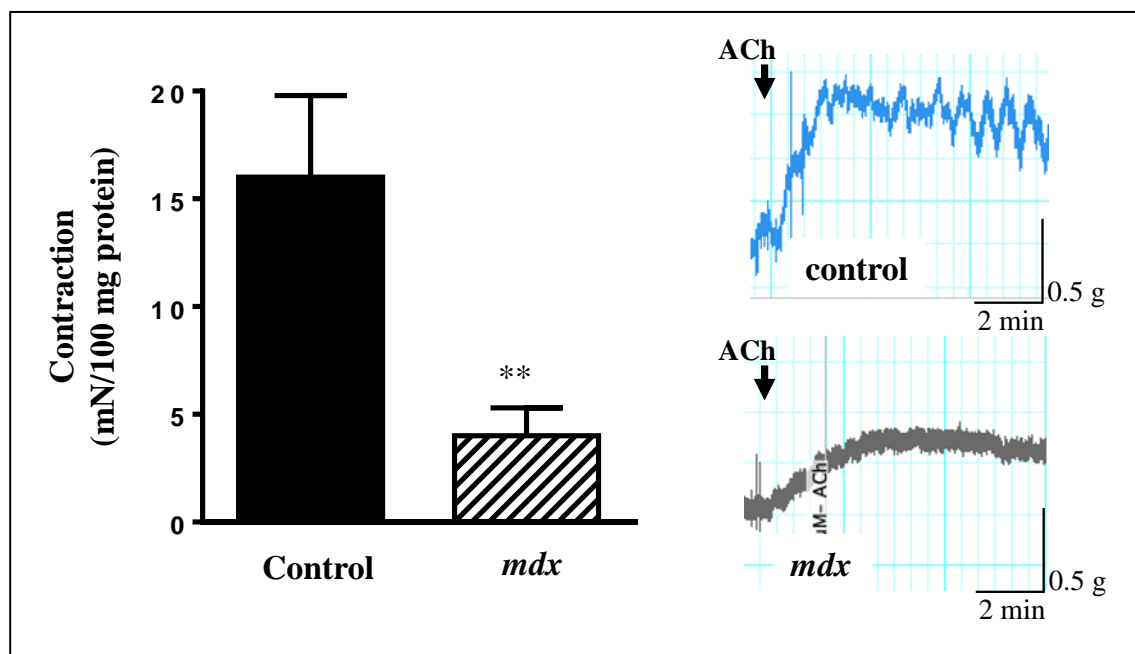


Figure 3. Colonic muscle strips were isolated from 3-month old control and *mdx* mice. Contraction in response to acetylcholine ($10 \mu\text{M}$) was measured in organ bath experiments. Contraction was recorded as increase in grams and calculated as $\text{mN}/100\text{g mg tissue}$. **Left panel:** Bar graphs of calculated values ($n=4-5$). **Right panel:** Representative tracing of acetylcholine-

*induced contraction in colonic muscle strips from control and mdx mice. Contraction was significantly decreased in mdx mice. ** $p < 0.05$, $n = 4-5$*

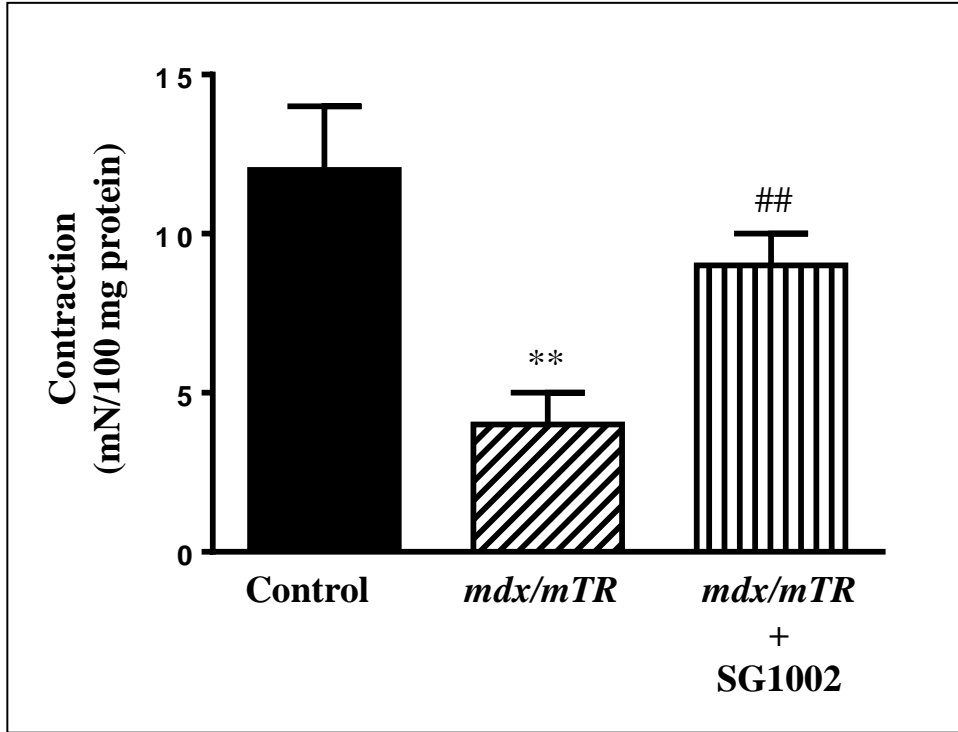


Figure 4. Colonic muscle strips were isolated from 9-month old control and mdx/mTR mice and mdx/mTR mice treated with SG1002, an orally active H₂S donor. Contraction in response to acetylcholine (10 μM) was measured in organ bath experiments. Contraction was recorded as increase in grams and calculated as mN/100g mg tissue. Contraction was significantly decreased in mdx/mTR (** p < 0.05, n=4). Treatment with SG1002 partly and significantly reversed the inhibition in contraction (## p < 0.05, n=4).

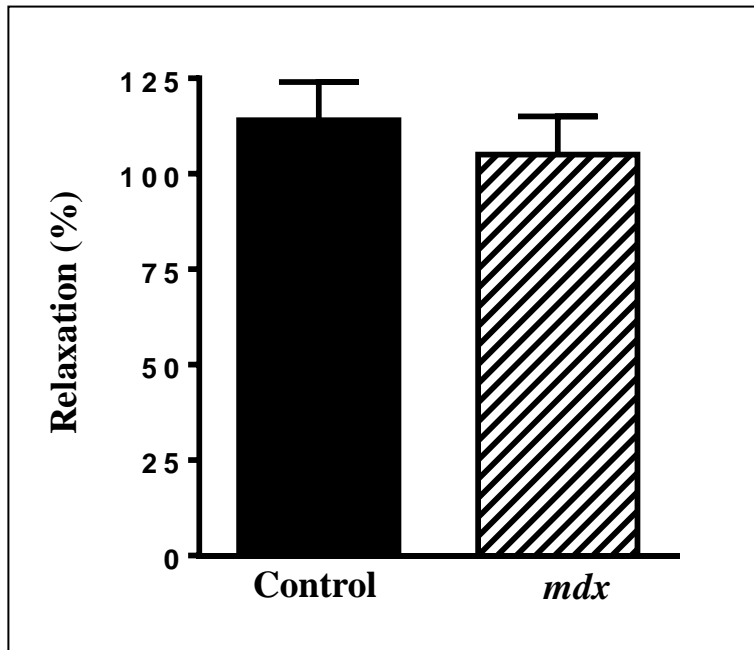


Figure 5. Colonic muscle strips were isolated from 3-month old control and mdx mice. Relaxation in response to nitric oxide donor, sodium nitroprusside (SNP, 10 μ M) was measured as inhibition of acetylcholine (10 μ M)-induced contraction and calculated as percent inhibition of contraction. SNP completely inhibited contraction in colonic muscle strips from both control and mdx mice (n=4-5)

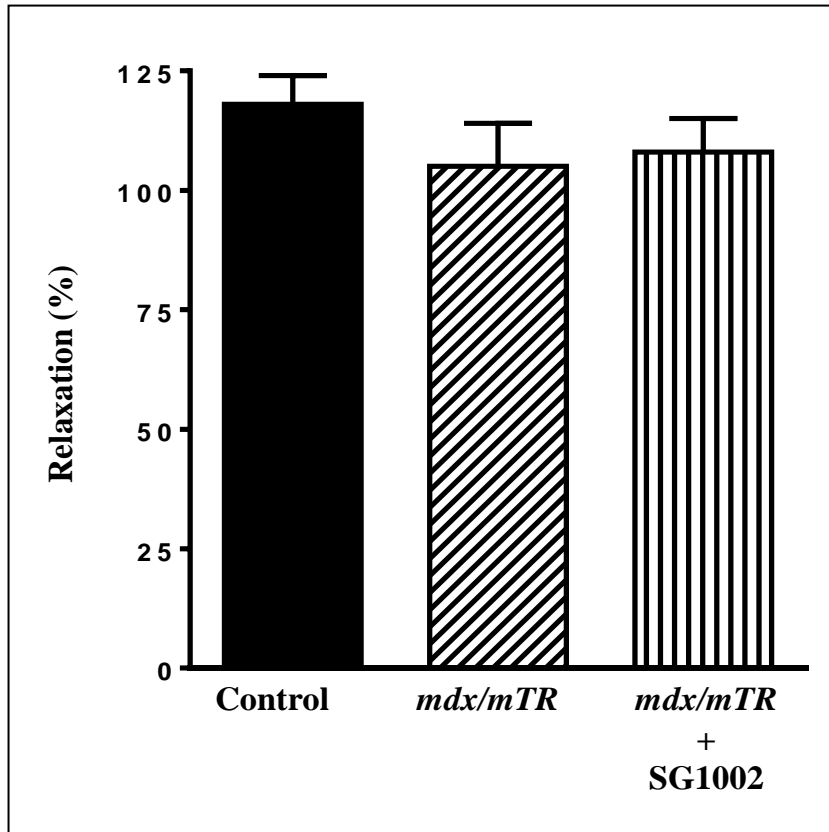


Figure 6. Colonic muscle strips were isolated from 9-month old control and mdx/mTR mice and mdx/mTR mice treated with SG1002, an orally active H₂S donor. Relaxation in response to nitric oxide donor, sodium nitroprusside (SNP, 10 μ M) was measured as inhibition of acetylcholine (10 μ M)-induced contraction and calculated as percent inhibition of contraction. SNP completely inhibited contraction in colonic muscle strips from control and mdx/mTR mice and in mdx/mTR mice treated with SG1002 (n=4)

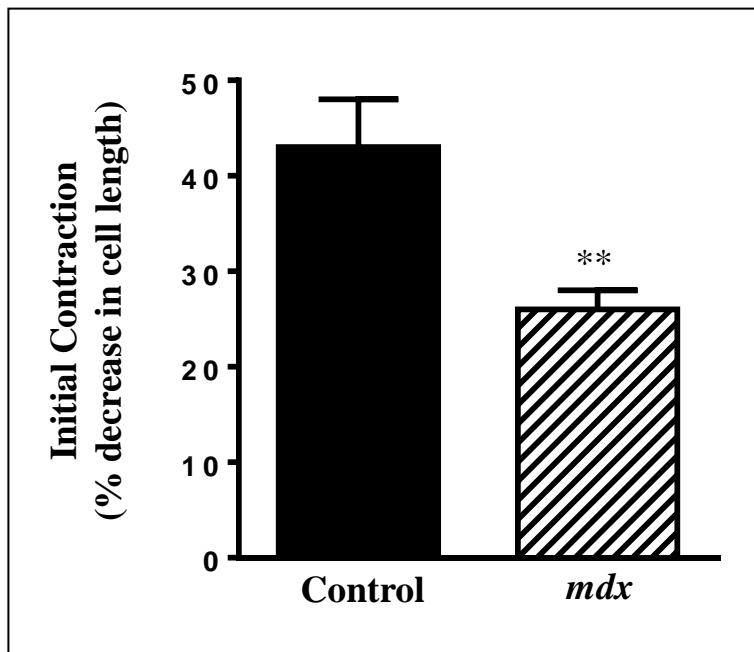


Figure 7. Smooth muscle cells were isolated from the colon of 3-month old control and mdx mice. Cells were treated with acetylcholine ($1 \mu\text{M}$) for 0.5 min and contraction was measured as decrease in cell length from the basal length (control: $68 \pm 4 \mu\text{m}$ and mdx: $64 \pm 6 \mu\text{m}$) and expressed as percent decrease in cell length. Initial contraction was significantly decreased in mdx mice.

** $p < 0.05$, $n = 4-5$

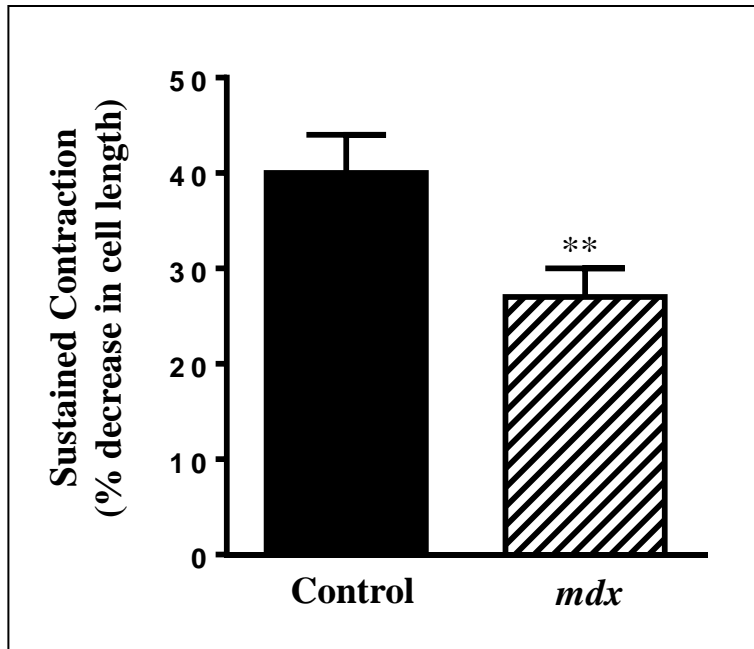


Figure 8. Smooth muscle cells were isolated from the colon of 3-month old control and mdx mice. Cells were treated with acetylcholine ($1 \mu\text{M}$) for 0.5 min and contraction was measured as decrease in cell length from the basal length (control: $68 \pm 4 \mu\text{m}$ and mdx: $64 \pm 6 \mu\text{m}$) and expressed as percent decrease in cell length. Sustained contraction was significantly decreased in mdx mice. ** $p < 0.05$, $n = 4-5$

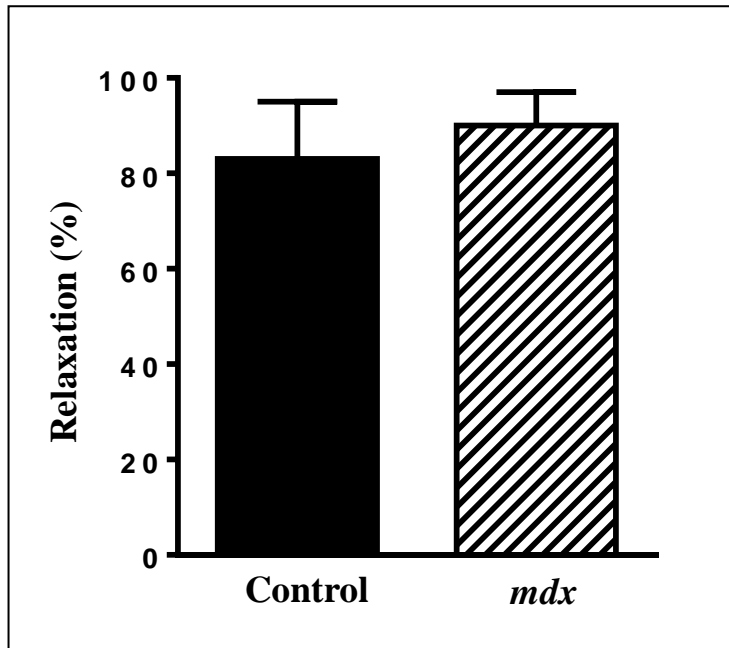


Figure 9. Smooth muscle cells were isolated from the colon of 3-month old control and mdx mice. Relaxation in response to nitric oxide donor, sodium nitroprusside (SNP, 10 μ M) was measured as inhibition of acetylcholine (1 μ M)-induced contraction and calculated as percent inhibition of contraction. SNP-induced relaxation was not different in colonic smooth muscle cells from both control versus mdx mice ($n=4-5$)

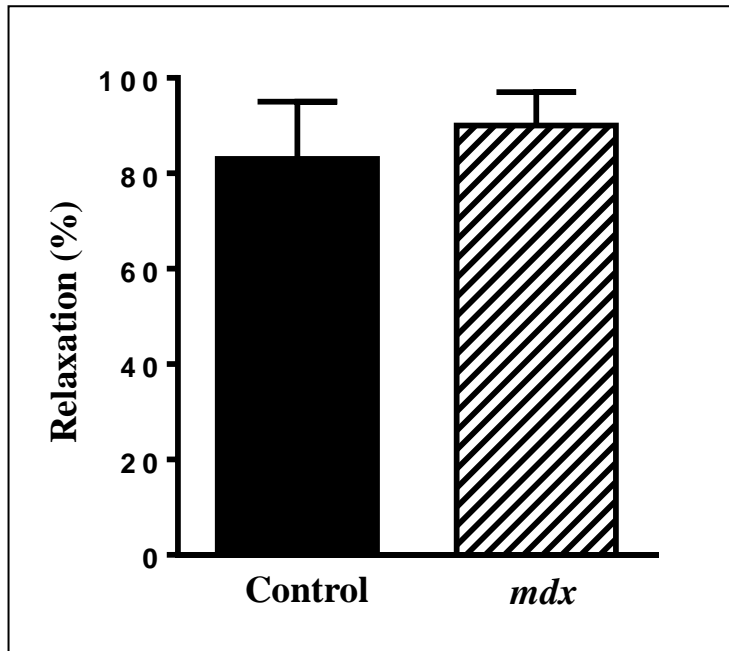


Figure 10. Smooth muscle cells were isolated from the colon of 3-month old control and mdx mice. Relaxation in response to β -adrenergic agonist isoproterenol ($10 \mu\text{M}$) was measured as inhibition of acetylcholine ($1 \mu\text{M}$)-induced contraction and calculated as percent inhibition of contraction. Isoproterenol-induced relaxation was not different in colonic smooth muscle cells from both control versus mdx mice ($n=4-5$)

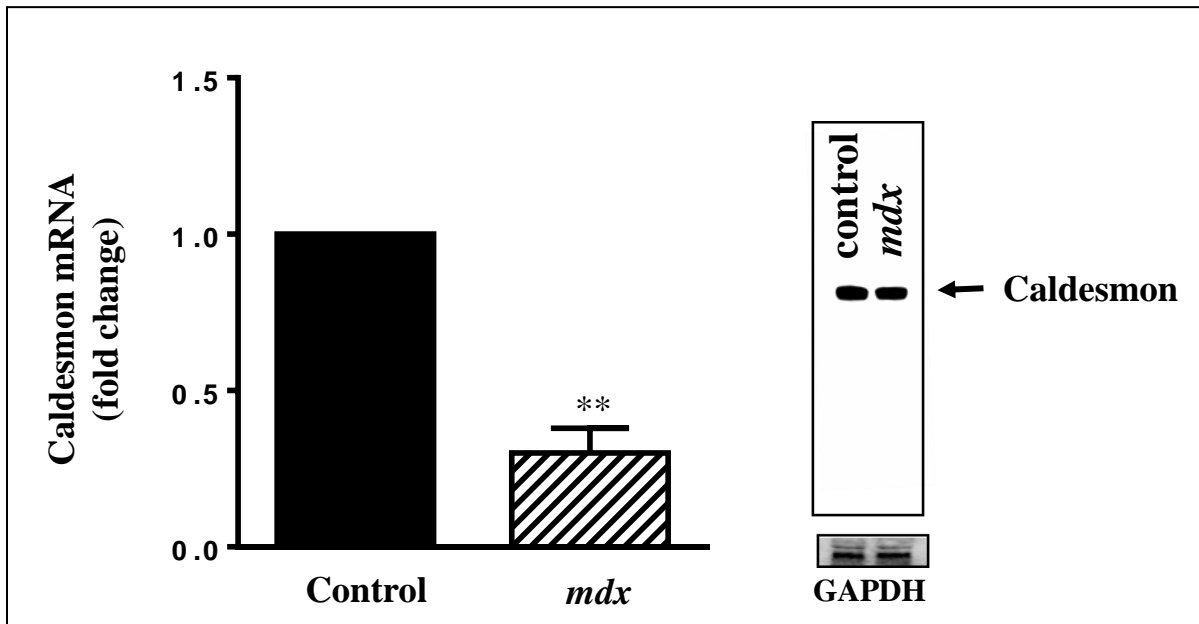


Figure 11. Expression of caldesmon in colonic smooth muscle of control and mdx mice Left Panel: RNA was isolated from colonic smooth muscle of 3-month old control and mdx mice. mRNA expression of caldesmon was measured using specific primers by quantitative RT-PCR and expressed as fold change over control. mRNA expression of caldesmon was significantly decreased in colonic smooth muscle from mdx mice compared to control (** $p < 0.05$, $n = 4-5$). Right panel: Lysates were prepared from colonic smooth muscle of control and mdx mice and expression of caldesmon was measured by western blot using specific antibody. Representative western blot image of 4 separate experiments was shown in the figure. Densitometry analysis of all the images showed no difference in the expression of caldesmon in colonic smooth muscle between control and mdx mice.

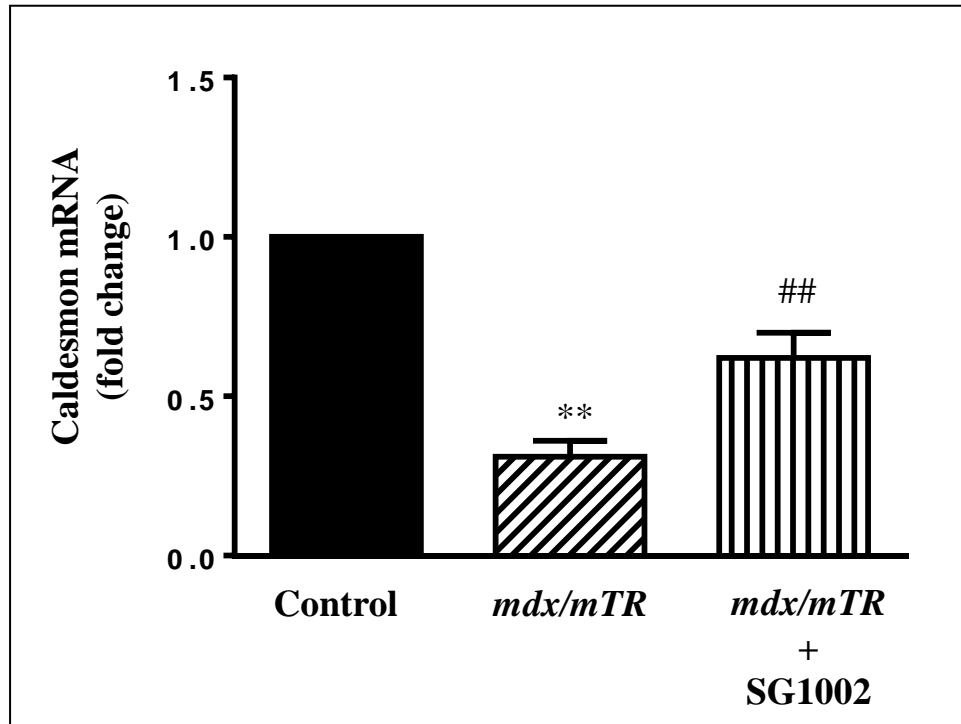


Figure 12. Effect of H₂S on caldesmon expression in colonic smooth muscle of mdx/mTR mice. Left Panel: RNA was isolated from colonic smooth muscle of 9-month old control and mdx/mTR mice and mdx/mTR mice treated with SG1002, an orally active H₂S donor mRNA expression of caldesmon was measured using specific primers by quantitative RT-PCR and expressed as fold change over control. mRNA expression of caldesmon was significantly decreased in colonic smooth muscle from mdx/mTR mice compared to control (** $p < 0.05$, $n = 4$). Treatment with SG1002 significantly reversed the inhibition in caldesmon mRNA expression (## $p < 0.05$, $n = 4$).

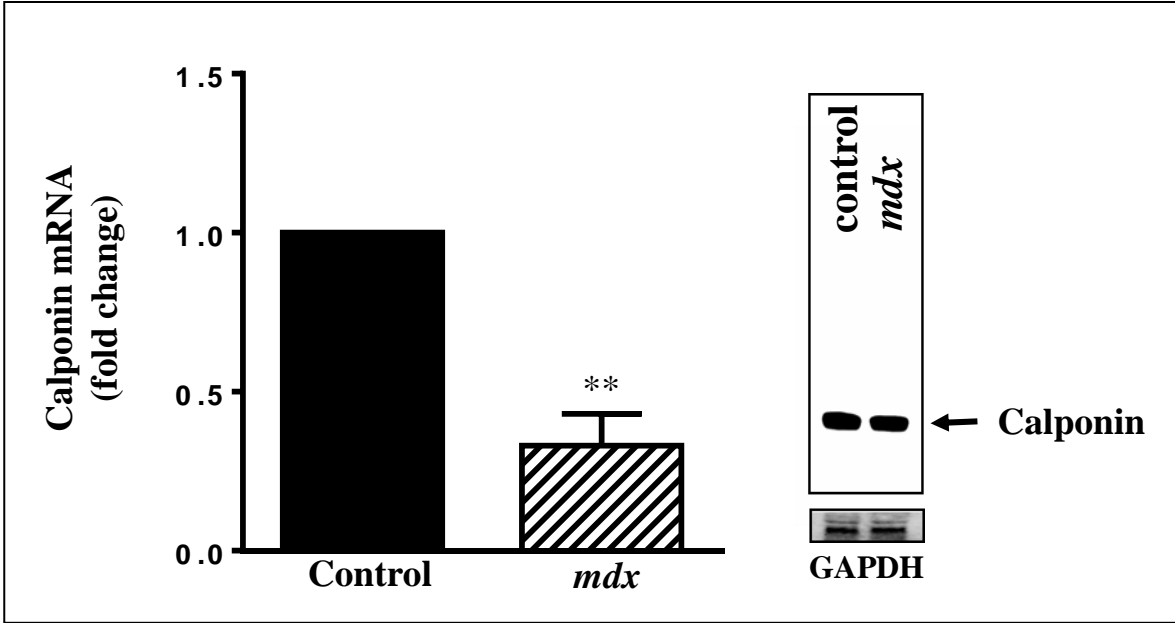


Figure 13. Expression of calponin colonic smooth muscle of control and mdx mice Left Panel: RNA was isolated from colonic smooth muscle of 3-month old control and mdx mice. mRNA expression of calponin was measured using specific primers by quantitative RT-PCR and expressed as fold change over control. mRNA expression of calponin was significantly decreased in colonic smooth muscle from mdx mice compared to control (** $p < 0.05$, $n = 4-5$). Right panel: Lysates were prepared from colonic smooth muscle of control and mdx mice and expression of calponin was measured by western blot using specific antibody. Representative western blot image of 4 separate experiments was shown in the figure. Densitometry analysis of all the images showed no difference in the expression of calponin colonic smooth muscle between control and mdx mice.

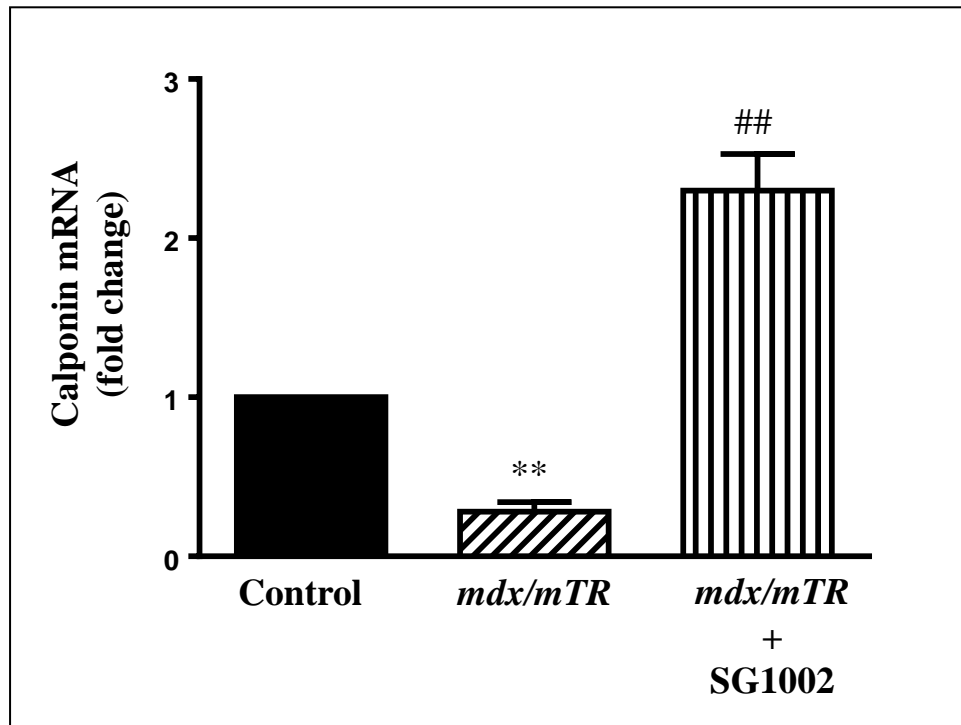


Figure 14. Effect of H_2S on calponin expression in colonic smooth muscle of mdx/mTR mice. Left Panel: RNA was isolated from colonic smooth muscle of 9-month old control and mdx/mTR mice and mdx/mTR mice treated with SG1002, an orally active H_2S donor mRNA expression of calponin was measured using specific primers by quantitative RT-PCR and expressed as fold change over control. mRNA expression of calponin was significantly decreased in colonic smooth muscle from mdx/mTR mice compared to control (** $p < 0.05$, $n = 4$). Treatment with SG1002 significantly reversed the inhibition in calponin mRNA expression (## $p < 0.05$, $n = 4$).

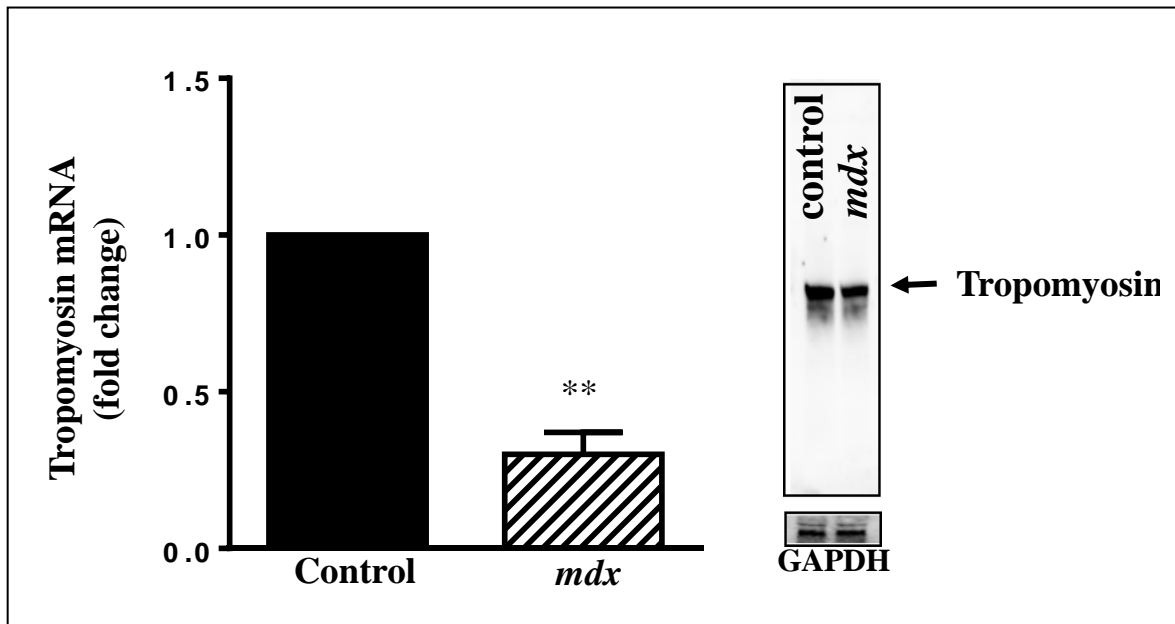


Figure 15. Expression of tropomyosin in colonic smooth muscle of control and mdx mice Left Panel: RNA was isolated from colonic smooth muscle of 3-month old control and mdx mice. mRNA expression of tropomyosin was measured using specific primers by quantitative RT-PCR and expressed as fold change over control. mRNA expression of tropomyosin was significantly decreased in colonic smooth muscle from mdx mice compared to control (** $p < 0.05$, $n = 4-5$). Right panel: Lysates were prepared from colonic smooth muscle of control and mdx mice and expression of tropomyosin was measured by western blot using specific antibody. Representative western blot image of 4 separate experiments was shown in the figure. Densitometry analysis of all the images showed no difference in the expression of tropomyosin in colonic smooth muscle between control and mdx mice.

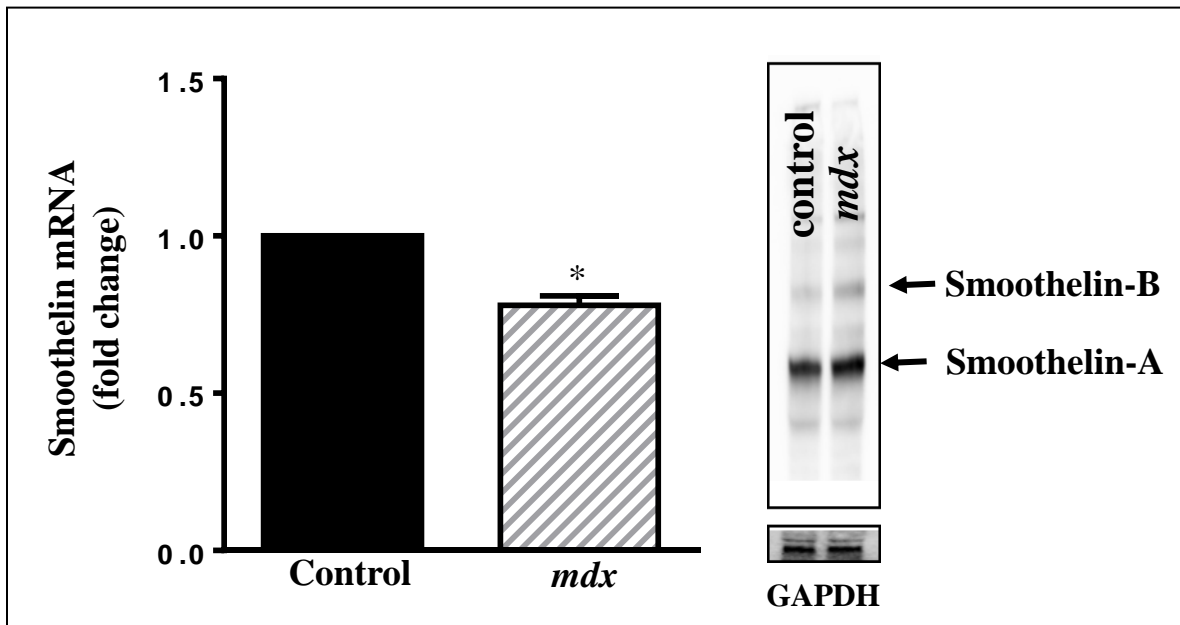


Figure 16. Expression of smoothelin in colonic smooth muscle of control and mdx mice Left Panel: RNA was isolated from colonic smooth muscle of 3-month old control and mdx mice. mRNA expression of smoothelin-A was measured using specific primers by quantitative RT-PCR and expressed as fold change over control. mRNA expression of smoothelin-A was significantly decreased in colonic smooth muscle from mdx mice compared to control (** $p < 0.05$, $n = 4-5$). Right panel: Lysates were prepared from colonic smooth muscle of control and mdx mice and expression of smoothelin was measured by western blot using specific antibody. Representative western blot image of 4 separate experiments was shown in the figure. Densitometry analysis of all the images showed no difference in the expression of smoothelin in colonic smooth muscle between control and mdx mice.

Chapter 4: DISCUSSION

Duchenne Muscular Dystrophy is the most common form of inherited muscular dystrophies that affects 1 in 3300 male births (Yucel et al., 2018). This genetic disorder is caused by a mutation in the gene located at Xp21 which encodes for the cytoskeleton protein dystrophin (Yucel et al., 2018). Dystrophin is present in all types of muscles and immunocytochemical studies have localized that dystrophin to the cytoplasmic surface of the plasma membrane associating tightly with a complex membrane glycoproteins. Because of its association with important structural proteins and sequence similarity with other structural proteins such as α -actinin, dystrophin is suggested to have an important structural role and provide resilience to the plasma membrane during contraction and relaxation. Dystrophin a large 427 kD protein. The dystrophin gene is transcribed into multiple RNA isoforms that show tissue specificity. Byers et al have shown that in SDS-PAGE, dystrophin characteristically appears as a doublet in skeletal and cardiac muscle suggesting different isoforms (Byers 1991). In contrast, dystrophin appears as a single band in intestinal smooth muscle. The levels of dystrophin in smooth muscle are lower compared to skeletal muscle (Byers 1991). Electron microscopy and immunofluorescence studies showed that dystrophin is specifically localized in caveolae this localization is distinct from the adherent junctions containing β 1 integrin, fibronectin and vinculin (Byers 1991) (North et al., 1993). Caveolae are microdomains of the plasma membrane that have been implicated in Ca^{++} homeostasis and signal transduction. The ability of caveolae to

sequester signaling components are due to the scaffolding properties of main caveolar protein, caveolin-1. Disruption of dystrophin-glycoprotein complex leads to increased permeability to Ca^{++} suggesting an important function of dystrophin in the regulation Ca^{++} homeostasis.

In smooth muscle, Ca^{++} and G protein-coupled receptor signaling are not only important for contraction, but also determine the cell phenotype. Caveolin-1 and the signaling molecules activated during contraction and relaxation of smooth muscle play an important in the regulation of expression of contractile protein and maintenance of contractile phenotype. Loss of caveolin-1 is associated with the decreased smooth muscle contraction and relaxation and change to proliferative phenotype (Halayko et al., 2005). The importance of caveolin-1 in signal transduction and its association with dystrophin highlights the significance of dystrophin in regulation of smooth muscle function.

Smooth muscle contains contractile apparatus consisting thin filaments as polymers of actin monomers and thick filaments as aggregates of myosin filaments. In addition, thin-filaments are associated with proteins such as calponin, caldesmon, tropomyosin and smoothelin. These proteins are shown to play a role in the regulation of acto-myosin interaction and contraction albeit the exact mechanism of regulation is not clear. For example, both calponin and caldesmon inhibit acto-myosin interaction and contraction, whereas smoothelin promotes contraction. Interaction of myosin and actin initiates cross-bridge cycling and this interaction is greatly facilitated by phosphorylation of 20 kDa myosin light chain (MLC_{20}). The levels of MLC_{20} phosphorylation of are regulated by MLC kinase and MLC phosphatase. Contractile agonists such as acetylcholine cause an

increase cytosolic Ca^{++} to stimulate Ca^{++} /calmodulin-dependent MLC kinase and a decrease in MLC phosphatase; both lead to increase in MLC_{20} phosphorylation.

Initially, DMD was considered predominantly a skeletal muscle disorder, clinically associated with symptoms such as progressive muscular wasting, waddling gait, pseudohypertrophy of the calves, and this overall loss of ambulation. Cardiac complications recently became more prominent, as cardiomyopathy and heart failure related mortality has increased. However, with advancing age, DMD patients also suffer from many gastrointestinal complications as well, such as bloating, gastroesophageal reflux, and highly prevalent, life threatening, constipation. These GI complications have not yet been systematically evaluated, and there is little scientific information on the pathophysiology and treatment of these conditions in DMD patients (Lo Cascio et al., 2016) (Petrof et al., 2002) (Shirokova and Niggli 2013). In DMD patients colonic dysmotility has been attributed to changes in the peristaltic wave patterns characteristic of the large intestine.

Colonic motility is regulated by enteric neurons, ICC and smooth muscle cells. In addition to the smooth muscle, dystrophin is expressed in enteric neurons and ICC (Vannuchhi et al., 2002). Abnormalities in nitrenergic neurotransmission have been suggested to play a role in altered colonic muscle contraction in innervated colonic muscle strips from *mdx* mice (Mule et al., 2010). To our knowledge, there are no studies on the role of dystrophin in the regulation of colonic smooth muscle function. In the present study we tested the hypothesis that dystrophin is essential for normal contraction and absence of dystrophin leads to changes in the expression of contractile proteins and decreased

contraction. The present study was undertaken to examine the role of dystrophin using isolated smooth muscle cells as well as muscle strips from colon of control and two DMD mouse models, *mdx* and *mdx/mTR*. Contraction in response to acetylcholine in muscle strips and isolated muscle cells from colon of both *mdx* and *mdx/mTR* mice was decreased compared to age-matched controls. Expression of calponin, caldesmon, tropomyosin and smoothelin mRNA was also decreased in colonic muscle from both *mdx* and *mdx/mTR* mice compared to age-matched controls. These results suggest that changes in smooth muscle function contributes, in addition to the altered neurotransmission, to altered gut motility in DMD. This is supported by our functional studies in isolated smooth muscle cells devoid of enteric neurons and ICC. However, given the expression of dystrophin in enteric neurons and ICC, we cannot exclude the participation of enteric neurons and ICC in the altered gut motility in DMD.

Another major finding of this study is that treatment of *mdx/mTR* mice with H₂S donor restores the mRNA of contractile proteins expression and contractile function similar or close to control. A novel H₂S drug, SG1002, has been recently introduced to attenuate myocardial cellular damage by increasing antioxidant products. Furthermore, in heart failure patients SG1002 was seen to increase circulatory bioavailability of NO and H₂S (Allen et al., 2010) (Chahbouni et al., 2010). It is unlikely the effect of H₂S is due to rapid effect on signaling pathways. The long-term treatment with H₂S points to its role as antioxidant and regulation of transcription factors such as Nrf2 that are involved in the anti-oxidation and anti-inflammation (Xie et al., 2016). Among the multiple pathogenic mechanisms proposed in DMD, oxidative stress and inflammation have been implicated in

the pathophysiology of disease. In support to this notion, recent studies by Boursereau et al (2018) have shown that NLRP3 inflammasome is involved in the pathogenesis of DMD and downregulation of NLRP3 inflammasome decreases DMD phenotype (Boursereau et al., 2018). Increase in the activities of NFAT, AP-1 and NF- κ B that play a role in inflammation are observed in dystrophic muscle (Evans et al., 2009). Another study showed that treatment of *mdx* mice with the anti-oxidant N-acetyl cysteine decreased oxidative stress and protected the muscle fiber from stretch-induced damage (Hori et al., 2011). Anti-oxidants such as melatonin and resveratrol have been used to ameliorate the muscular pathology by scavenging ROS in animal model of DMD (Biggar et al., 2001) (Merlini et al., 2003) (Wamhoff et al., 2006). More importantly, currently available treatment options for DMD are glucocorticoids and the most the significant effect of glucocorticoids is to inhibit expression of inflammatory genes.

In conclusion, our results demonstrate that in *mdx* and *mdx/mTR* mice mRNA expression of thin filament associated proteins are decreased and this is associated with decrease in smooth muscle contraction. Our results also demonstrate that treatment of *mdx/mTR* mice with H₂S donor restores expression of proteins and contraction in colonic smooth muscle. Our study suggests a therapeutic potential of SG1002 on the DMD phenotype. An important unanswered question remains: what is the effect of absence of dystrophin on the intrinsic signaling pathways activated by contractile agonists in smooth muscle cells? The lack of dystrophin is known to alter the Ca⁺⁺ homeostasis and hence it is hypothesized that Ca⁺⁺ regulated activity of MLC kinase and MLC₂₀ phosphorylation levels are also altered in *mdx* and *mdx/mTR* mice leading to decreased muscle contraction.

Finally, though it is clear dystrophin is an important plasma membrane protein that provides mechanical stability and its association caveolar proteins caveolin-1 might be important for contractile phenotype, future studies are required to elucidate the role of dystrophin in the signaling process that regulate smooth muscle contraction.

List of References

- 1) Allen, D., Gervasio, O., Yeung, E., & Whitehead, N. (2010). Calcium and the damage pathways in muscular dystrophy. *Canadian Journal Of Physiology And Pharmacology*, 88(2), 83-91.
- 2) Alves, G., Silva, L., Rosa, E., Aboulafia, J., Freymüller-Haapalainen, E., Souccar, C., & Nouailhetas, V. (2014). Intestine of dystrophic mice presents enhanced contractile resistance to stretching despite morphological impairment. *American Journal of Physiology. Gastrointestinal and Liver Physiology*, 306(3), G191-9.
- 3) Anastasi, G., Amato A., Tarone G., Vita G., Monici MC., Magauidda L., Cutroneo G. (2003). Distribution and Localization of Vinculin-Talin-Integrin System and Dystrophin-Glycoprotein Complex in Human Skeletal Muscle. *Cells Tissues Organs*, 175(3), 151-164.
- 4) Babu, G., Warshaw, D., Periasamy, M., Atkinson, Burr G., & Merrifield, Peter A. (2000). Smooth muscle myosin heavy chain isoforms and their role in muscle physiology. *Microscopy Research and Technique*, 50(6), 532-540.
- 5) Biggar, W., Gingras, M., Fehlings, D., Harris, V., & Steele, C. (2001). Deflazacort treatment of Duchenne muscular dystrophy. *Journal Of Pediatrics*, 138(1), 45-50.
- 6) Birnkrant, D., Bushby, K., Bann, C., Apkon, S., Blackwell, A., Brumbaugh, D., . . . Weber, D. (2018). Diagnosis and management of Duchenne muscular dystrophy, part 1: Diagnosis, and neuromuscular, rehabilitation, endocrine, and gastrointestinal and nutritional management. *The Lancet Neurology*, 17(3), 251-267.
- 7) Blake, D., Weir, A., Newey, S., & Davies, K. (2002). Function and genetics of dystrophin and dystrophin-related proteins in muscle. *Physiological Reviews*, 82(2), 291-329.

- 8) Boursereau, R., Abou-Samra, M., Lecompte, S., Noel, L., & Brichard, S. (2018). Downregulation of the NLRP3 inflammasome by adiponectin rescues Duchenne muscular dystrophy. *BMC Biology*, 16(1), BMC Biology, 12/2018, Vol.16(1).
- 9) Byers, T. (1991). The subcellular distribution of dystrophin in mouse skeletal, cardiac, and smooth muscle. *The Journal of Cell Biology*, 115(2), 411-421.
- 10) Chahbouni, M., Escames, G., Venegas, C., Sevilla, B., Garcia, J., Lopez, L., . . . Antonio Garcia, G. (2010). Melatonin treatment normalizes plasma pro-inflammatory cytokines and nitrosative/oxidative stress in patients suffering from Duchenne muscular dystrophy. *Journal Of Pineal Research*, 48(3), 282-289.
- 11) Evans, N., Misyak, S., Robertson, J., Bassaganya-Riera, J., & Grange, R. (2009). Immune-Mediated Mechanisms Potentially Regulate the Disease Time-Course of Duchenne Muscular Dystrophy and Provide Targets for Therapeutic Intervention. *Pm&R*, 1(8), 755-768.
- 12) Farah, C., & Reinach, F. (1995). The troponin complex and regulation of muscle contraction. *The FASEB Journal*, 9(9), 755-767.
- 13) Fulmer, T. (2011). New and improved dystrophic mice. *Science-Business EXchange*, 4(3), 65.
- 14) Guiraud, S., Aartsma-Rus, A., Vieira, N., Davies, K., Van Ommen, G., & Kunkel, L. (2015). The Pathogenesis and Therapy of Muscular Dystrophies. *Annual Review Of Genomics And Human Genetics*, Vol 16, 16, 281.
- 15) Gunst, S., & Tang, D. (2000). The contractile apparatus and mechanical properties of airway smooth muscle. *European Respiratory Journal*, 15(3), 600-616.
- 16) Halayko, A., & Stelmack, G. (2005). The association of caveolae, actin, and the dystrophinglycoprotein complex: A role in smooth muscle phenotype and function? *Canadian Journal of Physiology and Pharmacology*, 83(10), 877-891.
- 17) Han, R., Rader, E., Levy, J., Bansal, D., & Campbell, K. (2011). Dystrophin deficiency exacerbates skeletal muscle pathology in dysferlin-null mice. *Skeletal Muscle*, 1, Skeletal Muscle, 2011, Vol.1.
- 18) Holda, J., Klishin, A., Sedova, M., Huser, J., & Blatter, L. (1998). Capacitative calcium entry. *News In Physiological Sciences*, 13, 157-163.
- 19) Hori, Y., Kuno, A., Hosoda, R., Tanno, M., Miura, T., Shimamoto, K., & Horio, Y. (2011). Resveratrol Ameliorates Muscular Pathology in the Dystrophic mdx Mouse, a Model for

Duchenne Muscular Dystrophy. *Journal of Pharmacology and Experimental Therapeutics*, 338(3), 784-794.

- 20) Horowitz, A., Menice, C., Laporte, R., & Morgan, K. (1996). Mechanisms of smooth muscle contraction. *Physiological Reviews*, 76(4), 967-1003.
- 21) Kamdar, F., & Garry, D. (2016). Dystrophin-Deficient Cardiomyopathy. *Journal Of The American College Of Cardiology*, 67(21), 2533-2546.
- 22) Kaprielian, R., & Severs, N. (2000). Dystrophin and the cardiomyocyte membrane cytoskeleton in the healthy and failing heart. *Heart Failure Reviews*, 5(3), 221-38.
- 23) Kaprielian, R., Stevenson, S., Rothery, S., Cullen, M., & Severs, N. (2000). Distinct patterns of dystrophin organization in myocyte sarcolemma and transverse tubules of normal and diseased human myocardium. *Circulation*, 101(22), 2586-94.
- 24) Kimura, H. (2011). Hydrogen sulfide: Its production, release and functions. *Amino Acids*, 41(1), 113-21.
- 25) Kuo, I., & Ehrlich, B. (2015). Signaling in muscle contraction. *Cold Spring Harbor Perspectives in Biology*, 7(2), A006023.
- 26) Lim, K., Maruyama, R., & Yokota, T. (2017). Eteplirsen in the treatment of Duchenne muscular dystrophy. *Drug Design, Development and Therapy*, 11, 533-545.
- 27) Lo Cascio, C., Goetze, O., Latshang, T., Bluemel, S., Frauenfelder, T., & Bloch, K. (2016). Gastrointestinal Dysfunction in Patients with Duchenne Muscular Dystrophy. *Plos One*, 11(10), Plos One, 2016 Oct 13, Vol.11(10).
- 28) Lo Cascio, C., Latshang, T., Kohler, M., Fehr, T., & Bloch, K. (2014). Severe Metabolic Acidosis in Adult Patients with Duchenne Muscular Dystrophy. *Respiration*, 87(6), 499-503.
- 29) Mancardi, D., Penna, C., Merlino, A., Del Soldato, P., Wink, D., & Pagliaro, P. (2009). Physiological and pharmacological features of the novel gasotransmitter: Hydrogen sulfide. *Biochimica Et Biophysica Acta (BBA) - Bioenergetics*, 1787(7), 864-872.
- 30) Marchand, A., Abi-Gerges, A., Saliba, Y., Merlet, E., Lompré, A., & Islam, M. (2012). Calcium Signaling in Vascular Smooth Muscle Cells: From Physiology to Pathology. In *Calcium Signaling* (2012 ed., Vol. 740, Advances in Experimental Medicine and Biology, pp. 795-810). Dordrecht: Springer Netherlands.

- 31) Mcgreevy, J., Hakim, C., Mcintosh, M., & Duan, D. (2015). Animal models of Duchenne muscular dystrophy: From basic mechanisms to gene therapy. *Disease Models & Mechanisms*, 8(3), 195-213.
- 32) Merlini, L., Cicognani, A., Malaspina, E., Gennari, M., Gnudi, S., Talim, B., & Franzoni, E. (2003). Early prednisone treatment in Duchenne muscular dystrophy. *Muscle & Nerve*, 27(2), 222-227.
- 33) Misarkova, E., Behuliak, M., Bencze, J., & Zicha, E. (2016). Excitation-Contraction Coupling and Excitation-Transcription Coupling in Blood Vessels: Their Possible Interactions in Hypertensive Vascular Remodeling. *Physiological Research*, 65(2), 173-191.
- 34) Morgan, K., & Gangopadhyay, S. (2001). Invited review: Cross-bridge regulation by thin filament-associated proteins. *Journal of Applied Physiology (Bethesda, Md. : 1985)*, 91(2), 953-62.
- 35) Mourkioti, F., Kustan, J., Kraft, P., Day, J., Zhao, M., Kost-Alimova, M., . . . Blau, H. (2013). Role of telomere dysfunction in cardiac failure in Duchenne muscular dystrophy. *Nature Cell Biology*, 15(8), 895-U300.
- 36) Mule, F., Amato, A., & Serio, R. (2010). Gastric emptying, small intestinal transit and fecal output in dystrophic (mdx) mice. *Journal Of Physiological Sciences*, 60(1), 75-79.
- 37) Niessen, P., Rensen, S., Van Deursen, J., De Man, J., De Laet, A., Vanderwinden, J., . . . Van Eys, G. (2005). Smoothelin-ais essential for functional intestinal smooth muscle contractility in mice. *Gastroenterology*, 129(5), 1592-601.
- 38) North, A., Galazkiewicz, B., Byers, T., Glenney, J., & Small, J. (1993). COMPLEMENTARY DISTRIBUTIONS OF VINCULIN AND DYSTROPHIN DEFINE 2 DISTINCT SARCOLEMMA DOMAINS IN SMOOTH-MUSCLE. *Journal Of Cell Biology*, 120(5), 1159-1167.
- 39) Nowak, K., & Davies, K. (2004). Duchenne muscular dystrophy and dystrophin: Pathogenesis and opportunities for treatment. *EMBO Reports*, 5(9), 872-876.
- 40) Petkova, M., Morales-Gonzales, S., Relizani, K., Gill, E., Seifert, F., Radke, J., . . . Schuelke, M. (2016). Characterization of a Dmd EGFP reporter mouse as a tool to investigate dystrophin expression. *Skeletal Muscle*, 6, Skeletal Muscle, 2016, Vol.6.
- 41) Petrof, B. J. (2002). Molecular Pathophysiology of Myofiber Injury in Deficiencies of the Dystrophin-Glycoprotein Complex. *American Journal of Physical Medicine & Rehabilitation*, 81(11 Suppl), S162-S174.

- 42) Petrof, B., Shrager, J., Stedman, H., Kelly, A., & Sweeney, H. (1993). Dystrophin protects the sarcolemma from stresses developed during muscle contraction. *Proceedings of the National Academy of Sciences of the United States of America*, 90(8), 3710-4.
- 43) Ryder, S., Leadley, R., Armstrong, N., Westwood, M., De Kock, T., Butt, J., . . . Kleijnen, R. (2017). The burden, epidemiology, costs and treatment for Duchenne muscular dystrophy: An evidence review. *Orphanet Journal Of Rare Diseases*, 12, Orphanet Journal Of Rare Diseases, 2017 Apr 26, Vol.12.
- 44) Sarna, S. (2010). *Colonic motility from bench side to bedside* (Colloquium series on integrated systems physiology; #11). San Rafael, Calif.?: Morgan & Claypool Life Sciences.
- 45) Shirokova, & Niggli. (2013). Cardiac phenotype of Duchenne Muscular Dystrophy: Insights from cellular studies. *Journal of Molecular and Cellular Cardiology*, 58(1), 217-224.
- 46) Singh, S., & Lin, H. (2015). Hydrogen Sulfide in Physiology and Diseases of the Digestive Tract. *Microorganisms*, 3(4), 866-889.
- 47) Terrill, J., Radley-Crabb, H., Iwasaki, T., Lemckert, F., Arthur, P., & Grounds, M. (2013). Oxidative stress and pathology in muscular dystrophies: Focus on protein thiol oxidation and dysferlinopathies. *The FEBS Journal*, 280(17), 4149-64.
- 48) Vannucchi, M., Zardo, C., Corsani, L., & Fausone-Pellegrini, M. (2002). Interstitial cells of Cajal, enteric neurons, and smooth muscle and myoid cells of the murine gastrointestinal tract express full-length dystrophin. *Histochemistry And Cell Biology*, 118(6), 449-457.
- 49) Veigel, C., Molloy, J., Schmitz, S., & Kendrick-Jones, J. (2003). Load-dependent kinetics of force production by smooth muscle myosin measured with optical tweezers. *Nature Cell Biology*, 5(11), 980-986.
- 50) Walsh, M. (1994). Calmodulin and the regulation of smooth muscle contraction. *Molecular and Cellular Biochemistry*, 135(1), 21-41.
- 51) Wamhoff, B., Bowles, D., & Owens, G. (2006). Excitation-transcription coupling in arterial smooth muscle. *Circulation Research*, 98(7), 868-78.
- 52) Wang, R. (2012). Physiological implications of hydrogen sulfide: A whiff exploration that blossomed. *Physiological Reviews*, 92(2), 791-896.
- 53) Webb, R. (2003). Smooth muscle contraction and relaxation. *Advances In Physiology Education*, 27(4), 201-206.
- 54) Whiteman, M., Armstrong, J., Chu, S., Jia-Ling, S., Wong, B., Cheung, N., . . . Moore, P. (2004). The novel neuromodulator hydrogen sulfide: An endogenous peroxynitrite 'scavenger'? *Journal of Neurochemistry*, 90(3), 765-768.

- 55) Xie, LP., Gu, Y., Wen, Ml., Zhao, S., Wang, W., Ma, Y., . . . Ji, Y. (2016). Hydrogen Sulfide Induces Keap1 S-sulfhydration and Suppresses Diabetes-Accelerated Atherosclerosis via Nrf2 Activation. *Diabetes*, 65(10), 3171-3184.
- 56) Yucel, N., Chang, A., Day, J., Rosenthal, N., & Blau, H. (2018). Humanizing the mdx mouse model of DMD: The long and the short of it. *NPJ Regenerative Medicine*, 3(1), 4.